10-8-2004

Morphology of the prothorax and procoxa in the New World Cryptocephalini (Coleoptera: Chrysomelidae: Cryptocephalinae)

M. Lourdes Chamorro-Lacayo
University of Minnesota Saint-Paul, cham0138@umn.edu

Alexander S. Konstantinov
U.S. Department of Agriculture, c/o National Museum of Natural History, akon-stan@sel.barc.usda.gov

Zootaxa 676: 1–46 (2004)
www.mapress.com/zootaxa/

ISSN 1175-5326 (print edition)
ZOOTAXA
ISSN 1175-5334 (online edition)

676

Morphology of the prothorax and procoxa in the New World Cryptocephalini (Coleoptera: Chrysomelidae: Cryptocephalinae)

MARIA LOURDES CHAMORRO-LACAYO[1] & ALEXANDER S. KONSTANTINOV[2]

[1]*Department of Entomology, University of Minnesota, Saint-Paul, MN 55108, USA (email: cham0138@umn.edu);*

[2]*Systematic Entomology Laboratory, PSI, Agricultural Research Service, U.S. Department of Agriculture, c/o National Museum of Natural History, MRC 168, Washington, DC 20560, U.S.A. (email: akonstan@sel.barc.usda.gov).*

Table of contents

Abstract

The comparative morphology of the prothorax and procoxae of New World Cryptocephalini was studied based on representatives of 11 of the 13 genera of the tribe. This study revealed a set of characters of obvious diagnostic and possible phylogenetic value supporting the currently accepted generic classification and two subtribes instead of the three currently recognized. Two general types

Accepted by P.J. Johnson: 9 Sept. 2004; published: 8 Oct. 2004

of prothoracies were found, the first occurring in Cryptocephalina and Monachulina and the second in Pachybrachina. Previously undescribed for Polyphaga, a monocondylic joint between the coxa and trochantin, was found in all the genera studied. Possible movement of the trochanter, including the transfer of advance movement into rotation, is described and illustrated.

Keywords: Cryptocephalinae, prothorax, procoxa, comparative morphology, New World

Introduction

Cryptocephalini, are known as case-bearing leaf beetles, and are robust, cylindrical and compact beetles measuring between 2–7 mm long (Fig. 1). They can easily be distinguished from most beetles (including other leaf beetles) by the following features: head partially or completely concealed within the prothorax when viewed dorsally (hence their name); antennae filiform; base of the pronotum as wide as base of the elytra; seventh abdominal tergite usually visible beyond the elytra. The elytra of cryptocephalines bear distinct rows of punctures, which are sometimes useful diagnostically (White 1968). The sexes are easily separated by a deep, large, median, setose indentation in the female's seventh abdominal sternite. It is here where the egg is rotated while being coated in feces (Erber 1988).

Cryptocephalinae are currently divided into three tribes, Cryptocephalini, Chlamisini, and Clytrini (Reid 1995), previously regarded as subfamilies. Thirteen valid genera in three subtribes are presently recorded in New World Cryptocephalini: *Mastacanthus* Suffrian, *Sternoglossus* Suffrian, *Griburius* Haldeman, *Metallactus* Suffrian, *Pachybrachis* Chevrolat, and *Ambrotodes* Suffrian in subtribe Pachybrachina; *Heptarthrius* Suffrian, *Lexiphanes* Gistel, and *Stegnocephala* Baly in subtribe Monachulina; and *Cryptocephalus* Geoffroy, *Diachus* LeConte, *Bassareus* Haldeman, and *Triachus* LeConte in subtribe Cryptocephalina (Seeno & Wilcox 1982). For this study, specimens of *Mastacanthus* and *Sternoglossus* were not available due to their rarity in collections. Approximately 1,000 species of Cryptocephalini have been recorded in the New World (Blackwelder 1944, Riley et al. 2002, Wilcox 1975, White 1968), with *Cryptocephalus*, *Pachybrachis*, *Griburius*, *Lexiphanes* and *Metallactus* making up about 95% of the total diversity. This is merely an estimate of Cryptocephalini species diversity, as it is based on various general beetle checklists (Blackwelder 1944). The Cryptocephalinae fauna of the New World, excluding North America north of Mexico, is poorly known. Many genera have not been revised since they were initially described and many Neotropical species await description in museums and in the field.

The comparative morphology of Cryptocephalinae is not well studied. Some morphological data on cryptocephalines is available in comparative studies of certain structures or attributes of Chrysomelidae as a whole (Samuelson 1996), but in such studies usually only a few cryptocephaline genera were analyzed (Baccetti and Daccordi 1988, Suzuki 1988).

Other morphological data can be extracted from keys for identification (Lopatin 1977, Riley, et al. 2002). Among the structures used as sources for diagnostic characters, the prothorax is often mentioned. The relative width of the prosternum, structure of the pronotal base, and shape of the lateral margin are commonly used to separate taxa above the species level in both New and Old World faunas (Lopatin 1977, Riley, et al. 2002). However, no attempts have been made to describe the diversity of prothoracic features in the Cryptocephalini, including internal ridges of the prosternum, proendosternites, coxae, trochanters and trochantines. This paper treats the aforementioned structures in all but two (*Mastacanthus* and *Sternoglossus*, both belonging to Pachybrachina) valid New World Cryptocephalini genera.

Material and Methods

The beetles examined in this study were obtained from the chrysomelid collection at the National Museum of Natural History (USNM), Smithsonian Institution. We selected one or two species representatives from each genus found in different areas of the New World (see Appendix 1 for the list of examined species and their geographic data).

Beetles were initially softened in distilled water and subsequently cleared using 10% NaOH, either by soaking them overnight, or using a heat source to speed up the process. The prothorax was then separated from the rest of the body in a dissecting dish filled with distilled water. The head, meso- and metathoraces, and abdomen were stored in glycerin mixed with a small amount of ethanol. The remaining soft tissue in the prothorax was very carefully removed under a Zeiss Stemi SV 11 Apo dissecting microscope, ensuring integrity of the structures. The left leg, along with the trochantin and coxa, were removed after motion of the structures had been recorded. The prothorax was then cleaned in a detergent solution in an ultrasonic cleaner in preparation for the Scanning Electron Microscope (SEM). The prothorax, left procoxa and trochantin were then glued onto a stub and coated with a heavy metal. Images were taken with an AMRAY 1810 scanning electron microscope. In this paper we follow the morphological terminology of Snodgrass (1935), Hlavac (1972), and Larsén (1966) and terms for some muscles were taken from Baehr (1979). Other common terms, e.g. ventral appendage, lateral projection etc., were created based on the relative position of the morphological structures on the undissected beetle body.

Morphology

The main prothoracic differences separating the four beetle suborders occur in the pleura and trochantin, and how these are attached to each other (Hlavac 1972). In the suborders Archostemata, Myxophaga and Adephaga the pleuron is large and rigid and makes up part of the prothoracic wall. In Polyphaga the pleuron is reduced in size, internalized and

termed the endopleuron or cryptopleuron (Hlavac 1972, Larsén 1966, McHugh et al. 1997). In Archostemata the trochantin is external and movable, whereas in the Adephaga the trochantin is mobile but the pleuron and part of the sternum enclose the trochantin and a portion of the coxa. In Myxophaga and Polyphaga the trochantin and the pleura are fused. This fused structure, (trochantin-endopleuron) trochantino-cryptopleuron (Larsén 1966), is moved by the tergo-pleural muscle, which in turn moves the coxa (Larsén 1966). Coxal movement is also effected by the contraction of the episterno-coxal and epimero-coxal muscles (Larsén 1966).

The prothorax of Cryptocephalini, as that of other beetles, consists of a wide dorsal sclerite, the pronotum, and a much narrower ventral sclerite, the prosternum. As in all Polyphaga (Evans 1971, Lawrence and Britton 1994), the propleuron in cryptocephalines has become reduced, forming an endopleuron within the prothoracic cavity, which is attached to the trochantin. Anteriorly the pronotum and prosternum form a near perfectly rounded opening (Figs. 10, 22, 32, 41, 51, 62, 72, 89, 101, 109, 119) into which the beetle's head fits. The posterior opening is more complicated in shape, but always has a greater height than width (Figs. 4, 15, 23, 33, 42, 54, 63, 74, 83, 86, 92, 103, 110, 121, 132).

I. The pronotum

The pronotum is relatively convex, basally as wide as the elytra, and narrowing apically. It is distinctly margined laterally, apically and basally. In the Monachulina and Cryptocephalina the basal margin is strongly dentate (Figs. 3, 15, 19, 21, 50, 61, 64, 71, 73, 81, 82) except for *Diachus* and *Triachus* in which the denticles are greatly reduced (Figs. 31, 34, 40, 43). The basal margin is usually uniformly convex, being tallest medially, with a flat area across the mesoscutellum. However, in some Pachybrachina the basal margin of the pronotum is sinuate, being laterally as long as medially (Figs. 85, 88, 100, 108, 131). Ventrally from the basal margin, the pronotum forms a relatively short ridge flanking the basal opening. The border of the basal opening is margined and armed with two well separated longitudinal ridges in Monachulina and Cryptocephalina (Figs. 4, 15, 23, 33, 54, 63, 74, 83). Most Pachybrachina lack such ridges, but in some cases the border of the basal opening makes a relatively abrupt 'step' (Fig. 121). The pronotal surface is covered with punctures of various sizes. The antero- and posterolateral angles sometimes protrude and carry setiferous pores (Figs. 46, 47, 65, 66, 77, 79, 94, 95, 124, 125).

The ventral declivity of the pronotum, the hypomeron (Fig. 2), forms the lateral and part of the ventral wall of the prothorax and is usually less strongly punctured than the pronotum. The hypomeron is triangular in shape and is connected to the prosternum along the notosternal suture, located anterior to the procoxa. In Cryptocephalini the suture is not well developed. Its position can be recognized by a dramatic change of punctation of the surface. The prosternum is more coarsely punctured than the hypomeron (Figs. 2, 50), except in some Pachybrachina. The suture is clearly visible in the lateral corner of the pro-

coxal cavity (Figs. 2, 11, 68). The suture is also distinct inside the procoxal cavity, between the lateral and medial openings (Figs. 11, 26, 68, 93, 113). Posteriorly, beyond the procoxa, the hypomeron projects ventrally and meets the posterolateral projection of the intercoxal prosternal process. In most Cryptocephalini the apex of the hypomeron projection is cylindrical and has an opening into which the tip of the posterolateral part of the intercoxal prosternal process fits (Figs. 2, 13, 20, 63, 70). However, in many Pachybrachina the tip of the hypomeral projection and the connecting posterolateral part of the intercoxal prosternal process are dorsoventrally flattened (Figs. 86, 92, 103, 111).

Anterior to the hypomeral projection, further dorsally, deeper inside the prothoracic cavity and connected to internal (ventral) parts of the prosternum, lies a sclerotized arch (Fig. 4). It forms the ventral wall of the prothoracic cavity and bears two symmetrically placed appendages called apodemal apophyses (Snodgrass 1935) or furcal arms (Larsén 1966). By analogy with internal metathoracic ridges they can also be called proendosternites (Figs. 4, 14, 15). A portion of the sclerotized arch between the proendosternites was called the sternacosta by Snodgrass (1935). Whether the sternacosta, and arch as a whole (Fig. 4), is an extension of the hypomeron remains unclear. A lack of distinct sutures in this area prevents determination of borders between the sclerites.

There are three main possibilities as to the origin of the sternacosta: it could be formed either by the hypomeron, the prosternum, or a combination of both. Amongst these, the second possibility seems more justifiable, by reason of the location of the notosternal suture at the bottom of the coxal cavity. The presence of the notosternal suture may indicate that the structures situated ventral to the intercoxal prosternal process belong to the prosternum. The area at the beginning of the sternacosta, dorsal to the hypomeral projection, has several parallel wrinkles that may be interpreted as a connection of two different sclerites. Snodgrass (1935) did not comment on the specific origin of this sclerite, but the fact that it is discussed in the paragraph devoted to the prosternum undoubtedly reveals Snodgrass's thoughts on this matter. Accepting a prosternal origin would conserve existing terminology. Being attached to the sternacosta, proendosternites would have to be renamed if shown that the sternacosta or sclerotized arch is associated with the hypomeron.

II. The prosternum

A wide and relatively short sclerite, occupying the ventral part of the prothorax, is called the prosternum. The section of the prosternum between the procoxal cavities is the intercoxal prosternal process. Its shape and relative size varies greatly between Cryptocephalini taxa and it is an important source of, mostly generic level, characters. The anterior margin of the prosternum is usually uniformly concave, however, in some cryptocephalines it is convex medially and concave laterally, forming two elongate lateral projections (Fig. 21). The prosternal process is flat, but in males of some species it is armed with a relatively long 'horn' (Figs. 21, 24). The posterior margin of the intercoxal prosternal process is usu-

ally flat or concave and does not extend beyond the hypomeral projection in the Cryptocephalina and Monachulina (Figs. 9, 19, 21, 31, 40, 50, 61, 71, 81). The posterior margin is triangular or oval and usually extends beyond the hypomeral projection in most Pachybrachina (Figs. 100, 108) (not that pronounced in *Pachybrachis*, Figs. 85, 88).

Two main kinds of internal structures of the prosternum can be recognized in Cryptocephalini. In Cryptocephalina and Monachulina the posterior margin of the intercoxal prosternal process is bordered by a well developed internal ridge. The ridge is sometimes thickened medially (Figs. 4, 13, 20, 23, 37, 54, 70, 74, 83). The mesal part of the intercoxal prosternal process is flat with two internally directed lateral projections that are connected to the hypomeral projections. An opening between the basal part of the sternacosta and the aforementioned projection leads into the procoxal cavity (Figs. 11, 13, 25, 26, 68). The sternacosta is often situated just dorsal to the tip of the intercoxal prosternal process. The dorsal surface of the prosternum has a large opening which may lead to a medial opening of the procoxal cavity.

In Pachybrachina the posterior margin of the intercoxal prosternal process has no ridge and lies in one plane without ventrolateral projections (Figs. 86, 111, 121). Mesally the intercoxal prosternal process sometimes develops a denticle that inserts into a sharp invagination of the procoxal cavity, forming a medial articulation point for the coxal hinge (Fig. 93). The sternacosta lies deep within the prothoracic cavity, far from the tip of the intercoxal prosternal process (Figs. 86, 92, 103, 110, 123, 132). Relatively, the intercoxal prosternal process lies closer to the sternacosta in Cryptocephalina and Monachulina than it does in the Pachybrachina. The hypomeral projection is usually much wider in Pachybrachina and in some genera (e. g. *Griburius*) completely closes any opening into the procoxal cavity (Fig. 111). In *Ambrotodes* this opening is well developed (also relatively smaller than in the Cryptocephalina and Monachulina) (Figs. 121, 132), while in *Pachybrachis* it has the shape of a narrow crack (Figs. 86, 92). In Pachybrachina an opening on the dorsal surface of the prosternum is either small or invisible.

The proendosternites are two variously shaped appendages attached to the sternacosta of the prosternum, directed posteromedially into the prothoracic cavity. The base of each proendosternite is narrow and thick whereas the apex is wide and thin (Figs. 4, 14). They are symmetrically situated, almost exactly across from the connection of the hypomeron and the intercoxal prosternal process. According to Snodgrass (1935), the proendosternites support the principal longitudinal muscles of the thorax called M19 by Baehr (1979). Due to their relative simplicity, we did not find that the proendosternites provided any valuable diagnostic characters at the generic level.

III. The procoxal cavity
(Figs. 11, 26, 35, 68, 93, 113, 122)

Usually the procoxal cavity in Cryptocephalini is transverse in shape (Fig. 11), but in some genera it is nearly as wide as long (Fig. 26*)*. It is wider medially than laterally. The antero-

medial part of the bottom of the coxal cavity, the cryptosternum (Hlavac 1972), is formed by the prosternum (Figs. 2, 68). The posterolateral wall of the cavity is formed by the hypomeron. There are two main openings at the bottom of the coxal cavity. The lateral opening is the largest and almost completely occupies the lateral corner of the cavity. It is sometimes bordered anteromedially by a moderately raised ridge. The trochantin and attached endopleuron reach endolateral areas of the prothoracic cavity through this opening. The posterior edge of the opening, formed by the hypomeron, has a variously shaped ridge (Figs. 68, 113) normally obscured by the coxa. Posteromesal to the lateral opening, separated by a narrow bridge, is a second much smaller and more rounded opening. This opening is closed posteriorly (Fig. 111) in cryptocephaline beetles with wide hypomeral projections fitting exactly between the intercoxal prosternal process and the sternacosta of the prosternum. Our preparations did not allow us to see exactly where it leads in *Griburius*, but an obvious assumption is that it leads into the prothoracic cavity. In Cryptocephalina, Monachulina, and to a lesser degree in the rest of Pachybrachina, the opening also leads towards the posterior, so that the coxa can be seen above the sternacosta (Figs. 4, 37, 83). The bridge separating the lateral and medial opening usually has a well developed notosternal suture (Figs. 2, 68). Posteriorly the procoxal cavities are closed, or very narrowly open (only in the Pachybrachina), with the hypomeral projection joined to the posterolateral projection of the intercoxal prosternal process.

IV. The trochantin and endopleuron
(Figs. 5, 6, 16, 18, 28–30, 38–39, 56–58, 78, 105, 112, 117, 126)

The trochantin is the smallest sclerite of the prothorax. Homologically it has been traced to the coxopleurite, being its prearticular part in plecopterous insects (Snodgrass 1935). It is triangular in shape and the ventral (distal) edge of the trochantin rests on the lateral rim of the procoxa (Figs. 56–57). The posterior apex of the distal edge of the trochantin fits between the lateral coxal projection and the lateral rim. A visible group of stiff setae, the proprioreceptive organ, are sensitive to movement between the trochantin and the coxa (Figs. 56, 58). The anterior apex of the trochantin borders the lateral rim of the coxa and acts as a lever (Evans 1971). A few dissections allowed us to see a tendon attached to the anteroapical, ventral (distal) edge of the trochantin (Figs. 16, 18), a potential attachment site for the tergo-pleural muscle (Evans 1971). The proximal apex of the trochantin is directed dorsally along the endopleuron. The trochantin is externally visible, fitting into the lateral corner of the procoxal cavity (Figs. 44, 67, 104). The connection between the trochantin and the coxa is membranous, allowing for some articulation with what appears to be a monocondylic joint (Figs. 97, 105).The endopleuron is an internal remnant of the propleuron. It is attached to the internal surface of the trochantin and is situated in the lateral part of the procoxal cavity. It consists of a narrow stalk connected laterally to the trochantin (continuing further and apicomedially disappears into a large lateral opening in the coxa) and a wide “base” directed dorsally (Figs. 4, 36). According to Hlavac (1972) the

endopleuron provides increased surface area for muscle attachment. The endopleuron varies slightly in relative length of the stalk and greatly in width of the base in different Cryptocephalini.

V. The procoxa and trochanter
(Figs. 5–7, 16, 18, 28–30, 38–39, 48–49, 56–57, 59–60, 67, 69, 76, 78, 80, 84, 87, 96–99, 106–107, 112, 114–117, 126–130, 133–136)

Although the coxa is a basal leg segment, it forms a functional unity together with the prothorax, being positioned within the procoxal cavity and attached to the trochantin. The procoxa is globular in shape and has three openings. The large coxal opening is ventrally situated, inside the wide groove in which the apex of the trochanter and base of the profemur fit. The posterior aspect of the groove is equipped with a variously shaped projection. This projection, called the posterior projection below, fits into the indentation between the spiral ridge and the apical parts of the trochanter (Fig. 76). The coxal suture extends from the anterior margin of the ventral coxal opening to the much smaller dorsal opening (Figs. 5, 6, 16). When the coxa is positioned within the procoxal cavity, its ventral opening facing outward, the dorsal opening is hidden within the procoxal cavity (Figs. 52, 67, 76, 81). However, if the coxa is rotated towards the posterior, the dorsal opening can be observed (Figs. 27, 44). The medial aspect of the coxa is more or less uniformly convex. The lateral aspect is flattened and contains the largest opening, which can only be observed when the coxa is removed from the coxal cavity (Fig. 97). The rimmed side of this opening (the lateral coxal opening) has a tendon attached to it (Figs. 97–99). Several membranes attach the trochantin to this part of the coxa which bears a patch of stiff, short setae, termed proprioreceptive organs by Larsén (1966) (Fig. 17, 105). Terminal neurons of the receptors detect movement between the trochantin and the coxa, relaying back position, acceleration, and velocity information to the ganglia. Neurons in turn relay information to the muscles, allowing for a concerted movement of the insect (Chapman 1998). The anterior aspect of the ventral coxal groove forms a ridge which continues laterally forming a relatively long and curved projection (here termed lateral projection). This projection limits posterior movement of the trochantin. The coxal “ball”, of the monocondylic “ball and socket” joint of the trochantin and coxal articulation, is clearly visible in Figs. 49, 97, 105, 117. This joint is situated anteriad of the curved lateral projection and consists of a deep groove separating it from the lateral projection and the rim (part of it has proprioreceptive sensillae). The coxal tendon is situated nearly opposite this joint.

The trochanter has a complex shape (Figs. 7, 48, 60, 87, 106–107, 114, 129, 134). It fits into the procoxa running the entire length of the coxal suture, its wide ventrodistal aspect protruding from the ventral coxal opening and its narrow dorsoproximal aspect visible through the small dorsal opening of the procoxa (Figs. 27, 80). The profemur attaches to the wide, ventral aspect of the trochanter. An interesting feature of the trochanter is a spiral, transverse median ridge. When the trochanter is inserted into the coxa the ridge lies

on the coxal surface, where it slides when the trochanter rotates. The ventrally situated, posterior projection of the coxa is inserted between the wide, ventral end and the spiral ridge of the trochanter. Proprioreceptive sensillae cover the trochanteral surface between the wide, ventral apex and the spiral ridge, as well as the side of the dorsal aspect. A tendon is visible which attaches the dorsal aspect and the transverse spiral ridge of the trochanter (Figs. 7, 48, 60, 84, 114–116, 129–130). The trochanter of *Metallactus decumanus* clearly possesses a bifid dorsal aspect (Figs. 106–107). However, only one dorsal opening is present in the coxa. *Pachybrachis gayi* has only one dorsal aspect, similar to the other species studied, but a small subapical projection is also apparent (Fig. 87).

VI. Variability in prothoracic structures of New World Cryptocephalini
(see Appendix 2)

Our study of New World Cryptocephalini revealed a set of characters of obvious diagnostic and possible phylogenetic value. Distribution of these characters is described below.

MONACHULINA

PRONOTUM: Denticles present on basal margin (Figs. 54, 63, 74, 83); basal margin convex and truncate mesally, anteriad of mesoscutellum (Figs. 53, 64, 73, 82); pronotal punctures distinct all over or absent, strongly pronounced on all margins. HYPOMERON: Hypomeral projection cylindrical (Figs. 54, 63, 74, 83); hypomeron without apparent punctures (Figs. 50, 61, 71, 81). PROSTERNUM: Intercoxal prosternal process truncate or bimodal; intercoxal prosternal process with caudal M-shaped rim (Figs. 54, 70, 74, 83); prosternal opening wide, when viewed caudally (Figs. 54, 70, 74, 83); posterior margin of intercoxal prosternal process concave, never projecting beyond hypomeron (Figs. 50, 61, 71, 81); anterior margin of prosternum uniformly concave, with a medial flange, or with two submedial flanges (Figs. 50, 61, 71, 81); intercoxal width greater than width of coxal cavity. TROCHANTER: With a single dorsoproximal end (Figs. 60, 84).

Stegnocephala: Pronotal punctures absent (Figs. 71, 81). Intercoxal prosternal process truncate (Fig. 81); anterior margin of prosternum with a medial flange (Fig. 71), or two submedial flanges (Fig. 81).

Lexiphanes: Pronotal punctures distinct throughout (Fig. 64). Intercoxal prosternal process bimodal with small lateral projections (Fig. 62); anterior margin of prosternum uniformly concave (Fig. 61).

Heptarthrius: Pronotal punctures absent (Fig. 53). Intercoxal prosternal process bimodal (Fig. 51); anterior margin of prosternum uniformly concave (Fig. 50).

CRYPTOCEPHALINA

PRONOTUM: Denticles present (Figs. 15, 19, 23) or absent on basal margin (Figs. 33, 42); basal margin convex and mesally truncate over mesoscutellum (Figs. 9, 19, 23, 33, 42); pronotal punctures absent or distinct throughout, strongly pronounced on all margins.

HYPOMERON: Hypomeron projection cylindrical (Fig. 13); hypomeron without distinct punctures (Figs. 9, 12). PROSTERNUM: Intercoxal prosternal process truncate, bimodal or acutely bimodal; intercoxal prosternal process with caudal M-shaped rim (Figs. 13, 20); prosternal opening open, when viewd caudally; posterior margin of intercoxal prosternal process concave, never projecting beyond hypomeron (Fig. 9); anterior margin of prosternum uniformly concave or with medial flange; intercoxal width equal to, greater than, or less than width of coxal cavity.

Cryptocephalus: Denticles present on basal margin of pronotum (Figs. 15, 19); pronotal punctures distinct throughout (Figs. 10, 12). Intercoxal prosternal process acutely bimodal (Figs. 13, 20); anterior margin of prosternum uniformly concave or with medial flange; intercoxal width equal to or greater than width of coxal cavity (Figs. 9, 19).

Bassareus: Denticles present on basal margin of pronotum (Fig. 23); pronotal punctures distinct throughout (Figs. 23, 24). Intercoxal prosternal process bimodal (in males intercoxal prosternal process with medial projection) (Fig. 23); anterior margin of prosternum with medial flange (in males with sublateral indentations and lateral projections) (Fig. 21); intercoxal width equal to width of coxal cavity; without pronounced ridge bordering coxal cavity ending as small lateral projections on intercoxal prosternal process.

Triachus: Denticles absent on basal margin of pronotum (Figs. 40, 42); pronotal punctures absent (Fig. 43). Intercoxal prosternal process truncate (Fig. 40). Anterior margin of prosternum uniformly concave (Fig. 40); intercoxal width less than width of coxal cavity.

Diachus: Denticles absent on basal margin of pronotum (Figs. 31, 33); pronotal punctures absent (Fig. 34). Intercoxal prosternal process truncate. Anterior margin of prosternum uniformly concave; intercoxal width less than width of coxal cavity (Fig. 31).

PACHYBRACHINA

PRONOTUM: Denticles absent on basal margin (Figs. 85, 88, 100, 108, 118, 131); basal margin convex and sinusoidal, mesally truncate over mesoscutellum; pronotal punctures distinct throughout, strongly pronounced on all margins (Figs, 90, 102, 120). HYPOMERON: Hypomeral projection flat (Figs. 86, 91, 103, 111, 123); hypomeron with distinct punctures. PROSTERNUM: Prosternum similarly or more coarsely punctured than hypomeron; intercoxal prosternal process unimodal (Figs, 85, 88, 100, 108, 118, 122); intercoxal prosternal process without caudal M-shaped rim (Figs. 91, 103, 111, 123); prosternal opening narrowly open or closed in caudal view; posterior margin of intercoxal prosternal process convex, projecting beyond hypomeron (Figs. 85, 88, 100, 108, 118, 131); anterior margin of prosternum uniformly concave; intercoxal width equal to, greater than, or less than width of coxal cavity. TROCHANTER: With two dorsoproximal ends, with a subapical projection, or with only one dorsal end (Figs. 87, 106–107, 114–116, 128–130, 134–135).

Pachybrachis: Basal margin of pronotum sinusoidal (Figs. 85, 88). Prosternum and hypomeron equally coarsely punctured; prosternal opening closed in caudal view; anterior

margin of prosternum uniformly concave (Figs. 85, 88); intercoxal width less than width of coxal cavity. Trochanter with subapical projection on dorsoproximal end (Fig. 87)

Griburius: Basal margin of pronotum sinusoidal (Fig. 108). Prosternum more coarsely punctured than hypomeron; prosternal opening closed, in caudal view (Fig. 111); anterior margin of prosternum uniformly concave (Fig. 108); intercoxal width greater than width of coxal cavity. Trochanter with one dorsal end (Figs. 114–116).

Ambrotodes: Basal margin of pronotum sinusoidal (*A. signatipennis*) (Fig. 131) or convex and mesally truncate (*A. chilensis*) (Fig. 118). Prosternum more coarsely punctured than hypomeron; prosternal opening slightly open in caudal view (Figs. 121, 132); intercoxal cavity less than (*A. chilensis*) or greater than (*A. signatipennis*) width of coxal cavity. Trochanter with one dorsal end (Figs. 128–130).

Metallactus: Basal margin of pronotum sinusoidal (Fig. 100). Prosternum more coarsely punctured than hypomeron; prosternal opening closed, in caudal view (Fig. 103); intercoxal width equal to width of coxal cavity (Fig. 100). Trochanter with two dorsoproximal ends (Figs. 106–107).

Conclusions

Most of the sclerites of the prothorax have joined and are therefore immobile relative to each other, forming a structurally rigid body part. The only movable sclerites are the coxa with the attached trochantin and imbedded trochanter. Their movements determine the movement of the profemur. Due to the position of the articulation point on the intercoxal prosternal process, a horizontal hinge is formed. The procoxa has a limited ability to rotate around an axis between this point and the lateral corner of the procoxal cavity where the trochantin is attached. Articulation between the coxa and the trochantin is complicated. How the movement of the coxa translates into movement of the trochantin remains unclear. One articulation point between the coxa and the trochantin is obvious. It is formed by the lateral projection, impression and rim of the procoxa, and the posterior corner of the trochantin. This articulation point limits vertical movement of the trochantin and the attached endopleuron. Lawrence and Britton (1994) suggest that the coxa articulates with the trochantin at two points in the Polyphaga, however, we did not find the second point in the Cryptocephalini and therefore describe this joint as monocondylic (Figs. 49, 97, 105, 117).

Movement of the trochanter consists mainly of rotation along its own axis within the coxal cavity. This rotation allows the distal portion of the profemur and the rest of the leg a wide range of movement. Rotation of the trochanter is caused by contraction of a muscle attached to the trochanter tendon. If the tendon is attached to the trochanter longitudinally, it will pull the trochanter inside the coxal cavity causing its spiral ridge to slide along the coxal groove and the posterior projection of the coxa, hereby forcing the trochanter to rotate (Fig. 8). As we did not observe these movements, our description of transferred

advance movement into rotation is a hypothesis based on morphological observations. We also failed to find a tendon, indicative of muscle attachment to pull the trochanter in the opposite direction, causing it to return to its original position. However, the coxal cuticle may function as a spring, pushing the trochanter back after having been displaced by its own vertical movement. If the tendon were transversely attached to the trochanter then the associated muscle would rotate it upon contraction. The subsequent vertical movement, due to the position of the oblique spiral ridge, would transfigure the coxal cuticle, enabling to return the trochanter to its original position when the muscle relaxed. In the latter scenario, circular movement is transferred to advance movement. In both cases the vertical, or advance, movement of the trochanter inside the coxa is responsible for squeezing the coxa and eventually returning the trochanter to its original position. Therefore, the trochanter and coxa represent a device which transfers one kind of movement into another. However, whether the advance movements are being transferred into rotation or the opposite, remains unclear.

This study reveals a number of useful morphological characters that may supplement phylogenetic studies of the group and further clarify relationships at the generic level and beyond. Distribution of the main characters generally supports current generic classification of New World Cryptocephalini, but favors two family level taxa instead of the three currently recognized. Two main types of prothorax were found amongst the Cryptocephalini. The first type occurs in the Cryptocephalina and Monachulina. They share the following main character states (View Appendix 2 for table): cylindrical hypomeral projection; posterior margin of the intercoxal prosternal process not projecting beyond hypomeral projection; “three dimensional” intercoxal prosternal process with totally different internal prosternal structures, described in detail above (they include the internal ridge on the margin of the intercoxal prosternal process and some previously poorly described openings). They also have strongly dentate basal margin, with the exception of *Diachus* and *Triachus,* which we view as a secondary loss due to small body size. In Pachybrachina the hypomeral projection is flat; the posterior margin of the intercoxal prosternal process projects beyond hypomeral projection; flat intercoxal prosternal process and a number of unique features in the internal structures of prosternum; and in some genera a distinct trochanter. Without rigorous analysis of a variety of morphological structures we do not propose any formal changes to the higher classification of the Cryptocephalini, as this would be premature.

Generic level characters include the shape, details of margins, and surface structure of the pronotum, intercoxal prosternal process, as well as the relative width of the intercoxal prosternal process. The procoxa, trochantin, and to a lesser extent the trochanter, differ in small details which were impossible to qualify as well separated character states. These structures may prove useful at a higher level.

Acknowledgements

We are grateful to S. Braden and S. Whittaker (SEM Laboratory, National Museum of Natural History, Smithsonian Institution) for assisting with scanning electron microscopy. We are greatly thankful to M. Baehr (Zoologische Staatssammlung München), N. E. Woodley and A. N. Vandenberg (Systematic Entomology Laboratory, USDA, Washington, DC) and E. Grobelaar (Plant Protection Research Institute, Pretoria, South Africa) for reviewing this manuscript and providing valuable suggestions.

The senior author became interested in cryptocephalines while working with T. Erwin at the National Museum of Natural History, Smithsonian Institution, and finished this project while at the University of Minnesota as R. Holzenthal's advisee and being funded by NSF PEET grant number DEB-0117772, and is grateful for their support, enthusiasm, and encouragement.

Literature cited

Baccetti, B. & Daccordi, M. (1988) Sperm structure and phylogeny of the Chrysomelidae. *In*: Jolivet, P., Petitpierre, E. & Hsiao, H.H. (Eds.). *Biology of Chrysomelidae*. Kluwer Academic Publishers, Dordrecht/Boston/London, pp. 357–378.

Baehr, M. (1979) Vergleichende Untersuchungen am Skelett und an der Coxalmuskulatur des Prothorax der Coleoptera. Ein Beitrag zur Klärung der phylogenetischen Beziehungen der Adephaga (Coleoptera, Insecta). *Zoologica. Originalbhandlungen aus dem Gesamtgebiet der Zoologie*. 44. Band, 4. Lieferung, Heft 130. E. Schweizerbart'sche Verlagsbuchhandlung, Stuttgart, 76 pp.

Blackwelder, R.E. (1944) Checklist of the Coleopterous Insects of Mexico, Central America, the West Indies, and South America. *Smithsonian Institution, United States National Museum Bulletin*, 185(1–6), 639–647.

Chapman, R.F. (1998) *The Insects: Structure and Function*. 4th Edition. Cambridge University Press. United Kingdom, v–xvii + 770 pp.

Erber, D. (1988) Biology of Camptosomata Clytrinae, Cryptocephalinae, Chlamisinae, Lamprosomatinae, *In*: P. Jolivet, E. Petitpierre & Hsiao, T.H. (Eds.), *Biology of Chrysomelidae*. Kluwer Academic Publishers. Dordrecht, pp. 513–552.

Evans, M.E.G. (1971) Morphology and phylogeny in Coleoptera — the prothorax and procoxae. *International Congress of Entomology. XIII*, 1, 242–243.

Hlavac, T.F. (1972) The prothorax of Coleoptera: origin, major features of variation. *Psyche*, 79(3), 123–149.

Larsén, O. (1966) On the Morphology and Function of the Locomotor Organs of the Gyrinidae and other Coleoptera. *Opuscula Entomologica Supplement*, 30, 1–242.

Lawrence, J.F. & Britton, E.B. (1994) *Australian Beetles*. Melbourne University Press. 192 pp.

Lopatin, I.K. (1977) *Leaf beetles (Chrysomelidae) of Middle Asia and Kazakhstan*. "Nauka", Leningrad, 268 pp. (In Russian)

McHugh, J.V., C. J. Marshall, F. L. Fawcett. 1997. A Study of Adult Morphology in *Megalodacne heros* (Say) (Coleoptera: Erotylidae). *Transactions of the American Entomological Society*, 123 (4), 167–223.

Riley, E.G., Clark, S.M., Flowers, R.W. & Gilbert, A.J. (2002) 124. Chrysomelidae Latreille 1802. *In*: Arnett, R. H., Thomas, M.C., Skelley, P.E. & Frank, J.H. (Eds.), *American Beetles. Volume*

2. CRC Press. Boca Raton, London, New York, Washington, D.C., pp. 617–691.

Reid, C.A.M. (1995) A Cladistic Analysis of Subfamilial Relationships in the Chrysomelidae *sensu lato* (Chrysomeloidea). *In*: Pakaluk, J. & Slipinski, S.A. (eds.) *Biology, phylogeny, and classification of Coleoptera: Papers Celebrating the 80th Birthday of Roy A. Crowson*. Muzeum I Instytut Zoologii PAN, Warszawa, pp. 559–631.

Samuelson, G. A. (1996) Binding sites: elytron-to-body meshing structures of possible significance in the higher classification of Chrysomeloidea. *In:* Jolivet, P.H.A. & Cox, M.L. (eds.), *Chrysomelidae Biology. Volume 1: The Classification, Phylogeny and Genetics*. SPB Academic Publishing bv. The Netherlands, pp. 267–290.

Seeno, T.N. & Wilcox, J.A. (1982) Leaf Beetle Genera (Coleoptera: Chrysomelidae). *Entomography*, 1, 1–221.

Snodgrass, R.E. (1935) *Principles of Insect Morphology.* McGraw-Hill Book Company, Inc. New York and London, 667 pp.

Suzuki, K. (1988) Comparative morphology of the internal reproductive system of the Chrysomelidae. *In*: Jolivet, P., Petitpierre, E. & Hsiao, H.H. (Eds.), *Biology of Chrysomelidae*. Kluwer Academic Publishers, Dordrecht/Boston/London, pp. 317–355.

White, R.E. (1968) A Review of the Genus *Cryptocephalus* in America North of Mexico (Chrysomelidae: Coleoptera). *United States National Museum Bulletin*, 290, 1–124.

Wilcox, J.A. (1975) *Checklist of the Chrysomelidae of Canada, United States, Mexico, Central America and the West Indies.* North American Beetle Fauna Project. Red Version.Biological Research Institute, NY, 166 pp.

APPENDIX 1. List of Cryptocephalini for which SEM images were taken.

Subtribe	Genus	Species	Author	Country
Cryptocephalina	*Bassareus*		Haldeman	
		B. brunnipes	(Olivier)	Florida, USA
	Cryptocephalus		Geoffroy	
		C. arizonicus	Schaeffer	Arizona, USA
		C. aulicus	Haldeman	Florida, USA
	Diachus		LeConte	
		D. auratus	(Fabricius)	Guatemala
	Triachus		LeConte	
		T. vacuus	LeConte	Maryland, USA
Monachulina	*Heptarthrius*		Suffrian	
		H. longimanus	Suffrian	Perú
	Lexiphanes		Gistel	
		L. coenobita	Suffrian	Brazil
	Stegnocephala		Baly	
		S. discoidalis	Baly	Argentina
		S. costulata	(Suffrian)	Brazil
Pachybrachina	*Ambrotodes*		Suffrian	
		A. chilensis	(Blanchard)	Argentina
		A. signatipennis	(Blanchard)	Argentina
	Griburius		Haldeman	
		G. sp.		Mexico
	Metallactus		Suffrian	
		M. albopictus	Suffrian	Brazil
		M. decumanus	Suffrian	Brazil
	Pachybrachis		Chevrolat	
		P. gayi	Blanchard	Chile
		P. hepaticus	Melsheimer	California

APPENDIX 2. Variability in prothoracic structures of New World Cryptocephalini.

TAXA	PRONOTUM			HYPOMERON	
CRYPTOCEPHALINI	Denticles	Basal margin	Pronotal punctures	Hypomeron projection	Punctures
MONACHULINA	Present	Convex, mesally truncate		Cylindrical	Not apparent
S. costulata			Not apparent		
S. discoidalis			Not apparent		
Lexiphanes			Distinct		
Heptarthrius			Not apparent		
CRYPTOCEPHALINA					
C. aulicus	Present		Distinct		
C. arizonicus					
Bassareus	Present		Distinct		
Triachus	Absent		Not apparent		
Diachus	Absent		Not apparent		
PACHYBRACHINA	Absent		very distinct	Flat	Distinct
Pachybrachis		Sinusoidal			
Griburius		Sinusoidal			
A. chilensis		Convex, mesally truncate			
A. signatipennis		Sinusoidal			
Metallactus		Sinusoidal			

APPENDIX 2 (continued).

TAXA	INTERCOXAL PROSTERNAL PROCESS			
CRYPTOCEPHALINI	Shape	Caudal M-shaped Rim	Prosternal opening	Posterior margin
MONACHULINA		Present	Open	Concave, not projecting beyond hypomeron
S. costulata	Truncate			
S. discoidalis	Truncate			
Lexiphanes	Bimodal			
Heptarthrius	Bimodal			
CRYPTOCEPHALINA				
C. aulicus	Bimodal			
C. arizonicus				
Bassareus	Bimodal			
Triachus	Truncate			
Diachus	Truncate			
PACHYBRACHINA	Unimodal	Absent		Convex
Pachybrachis			Closed	
Griburius			Closed	
A. chilensis			Open	
A. signatipennis			Open	
Metallactus			Closed	

APPENDIX 2 (continued).

TAXA	PROSTERNUM		TROCHANTER
CRYPTOCEPHALINI	Anterior margin	Intercoxal width	Proximal ends
MONACHULINA		Greater than width coxal cavity	One
S. costulata	2 flanges		
S. discoidalis	1 medial		
Lexiphanes	Concave		
Heptarthrius	Concave		
CRYPTOCEPHALINA			
C. aulicus	Concave	Equal to	
C. arizonicus	1 medial	Greater than	
Bassareus	1 medial	Equal to	
Triachus	Concave	Less than	
Diachus	Concave	Less than	
PACHYBRACHINA	Concave		
Pachybrachis		Less than	Subapical projection
Griburius		Greater than	One
A. chilensis		Less than	One
A. signatipennis		Greater than	One
Metallactus		Equal to	Two

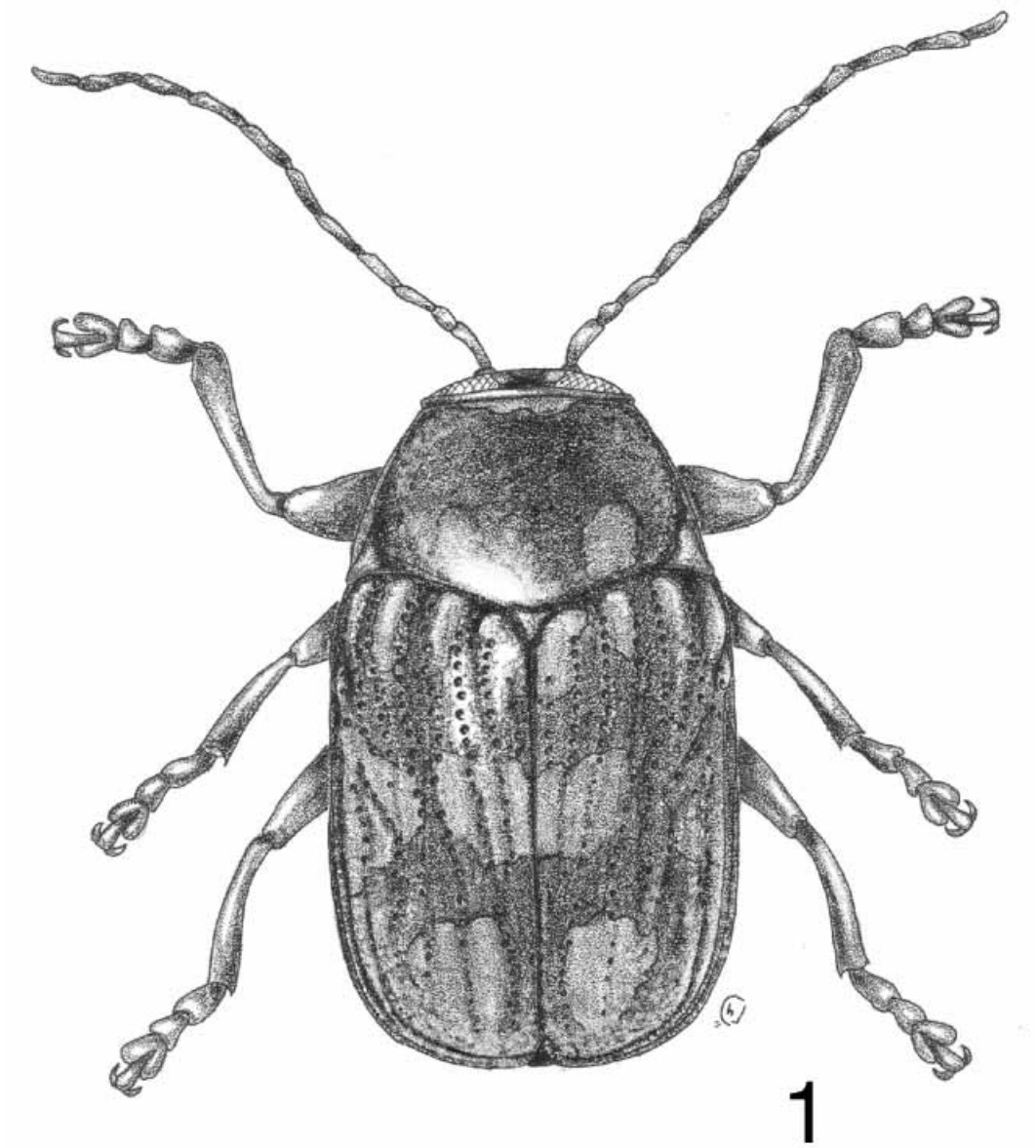

FIGURE 1. Habitus of *Bassareus brunnipes*.

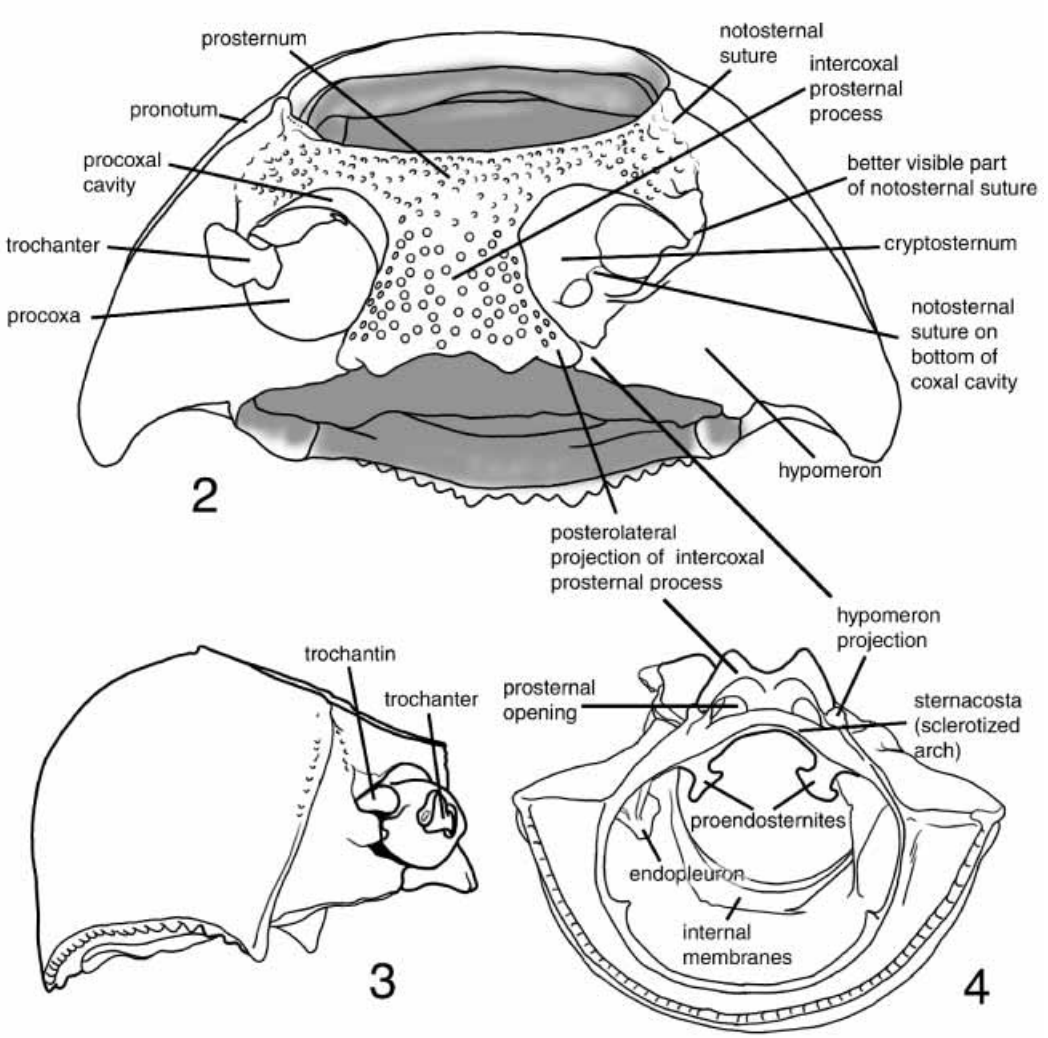

FIGURES 2–4. Schematic representation of *Cryptocephalus aulicus*. prothorax. 2, Ventral view. 3, Lateral view. 4, Caudal view.

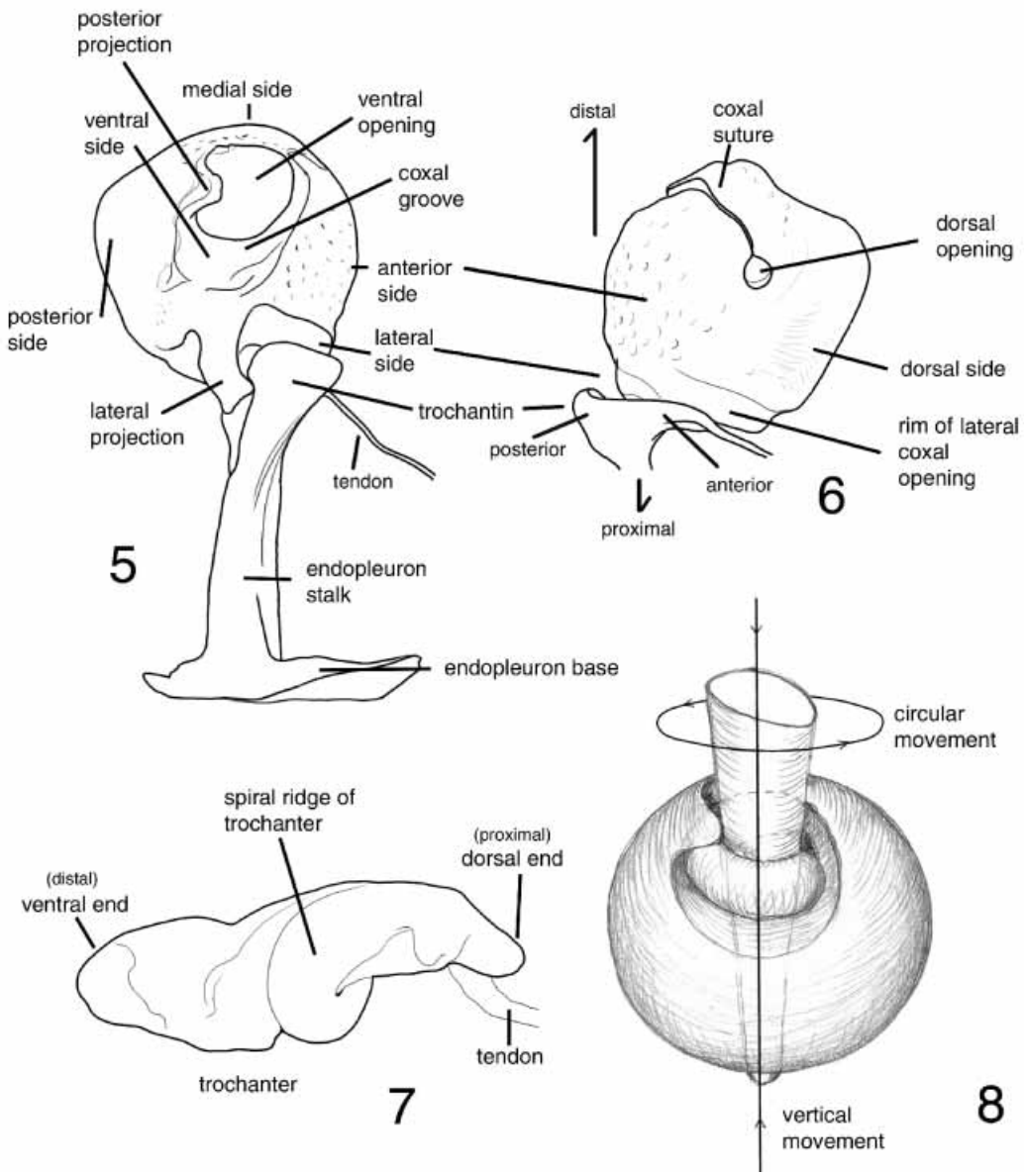

FIGURES 5–8. Schematic representation of *Cryptocephalus aulicus*. 5, Ventral aspect of coxa with attached trochantin and endopleuron. 6, Dorsal aspect of coxa with attached trochantin. 7, Trochanter. 8, Diagrammatic representation of trochanter movement within coxa.

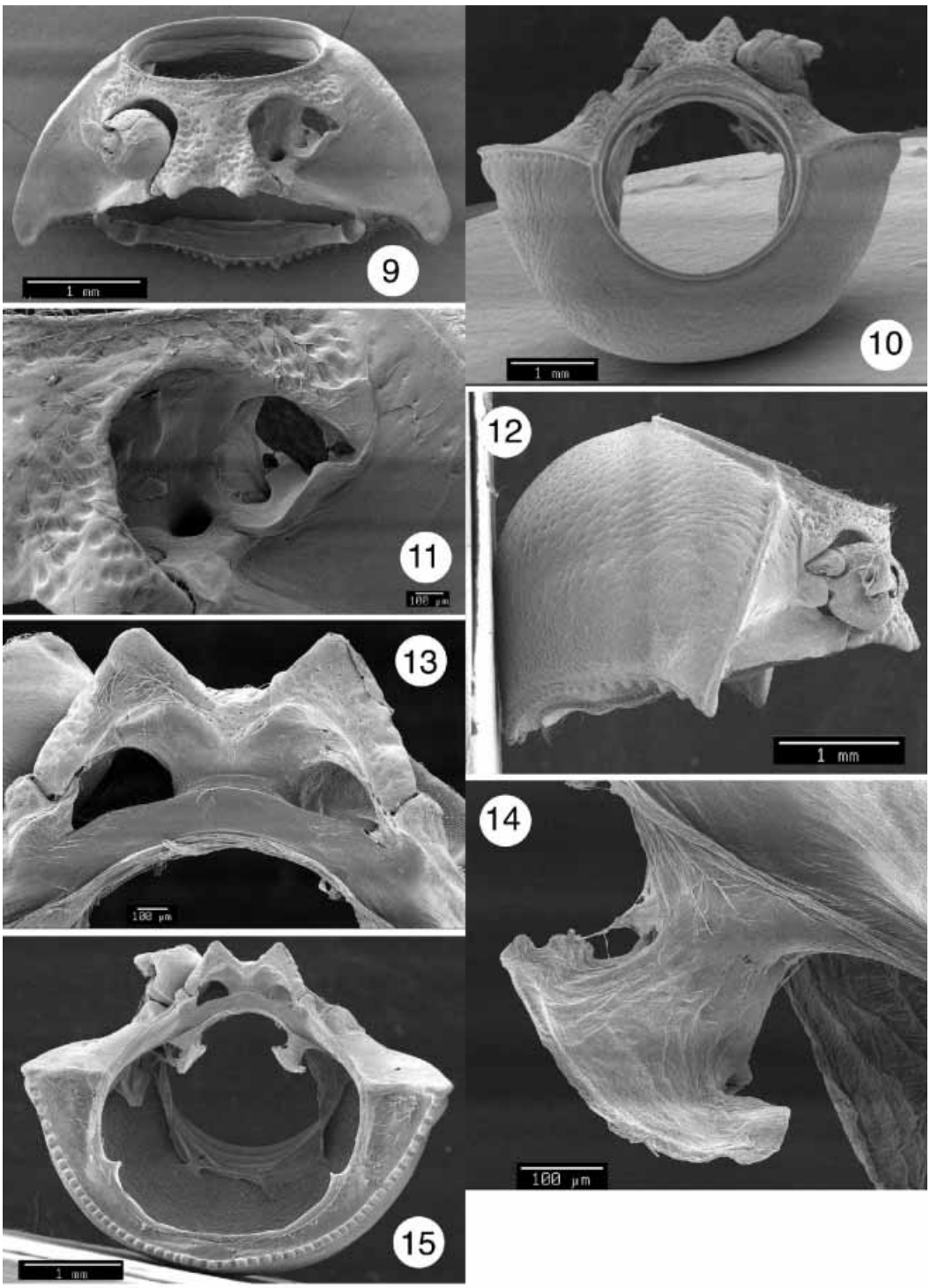

FIGURES 9–15. *Cryptocephalus aulicus*. 9, Ventral view of prothorax. 10, Anterior view. 11. Ventral view of coxal cavity. 12, Lateral view. 13, Caudal view of intercoxal prosternal process and sternacosta. 14, Proendosternite. 15, Caudal view.

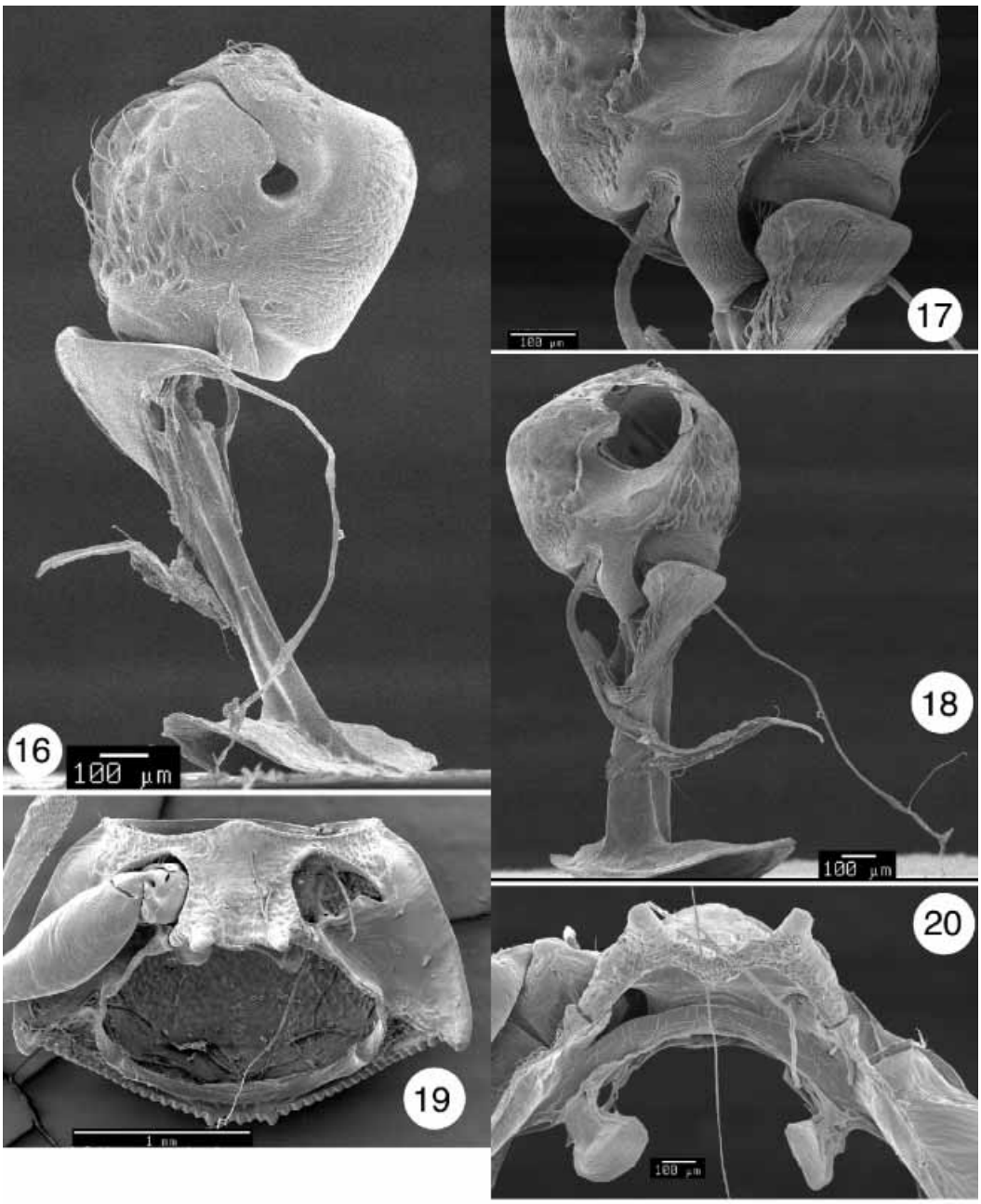

FIGURES 16–20. *Cryptocephalus aulicus*. 16, Dorsal aspect of coxa, trochantin, and endopleuron. 17, Caudal view of lateral projection of coxa. 18, Ventral aspect of coxa, trochantin, and endopleuron. **Figures 19–20.** *Cryptocephalus arizonicus*. 19, Ventral view of prothorax. 20, Caudal view of intercoxal prosternal process and sternacosta.

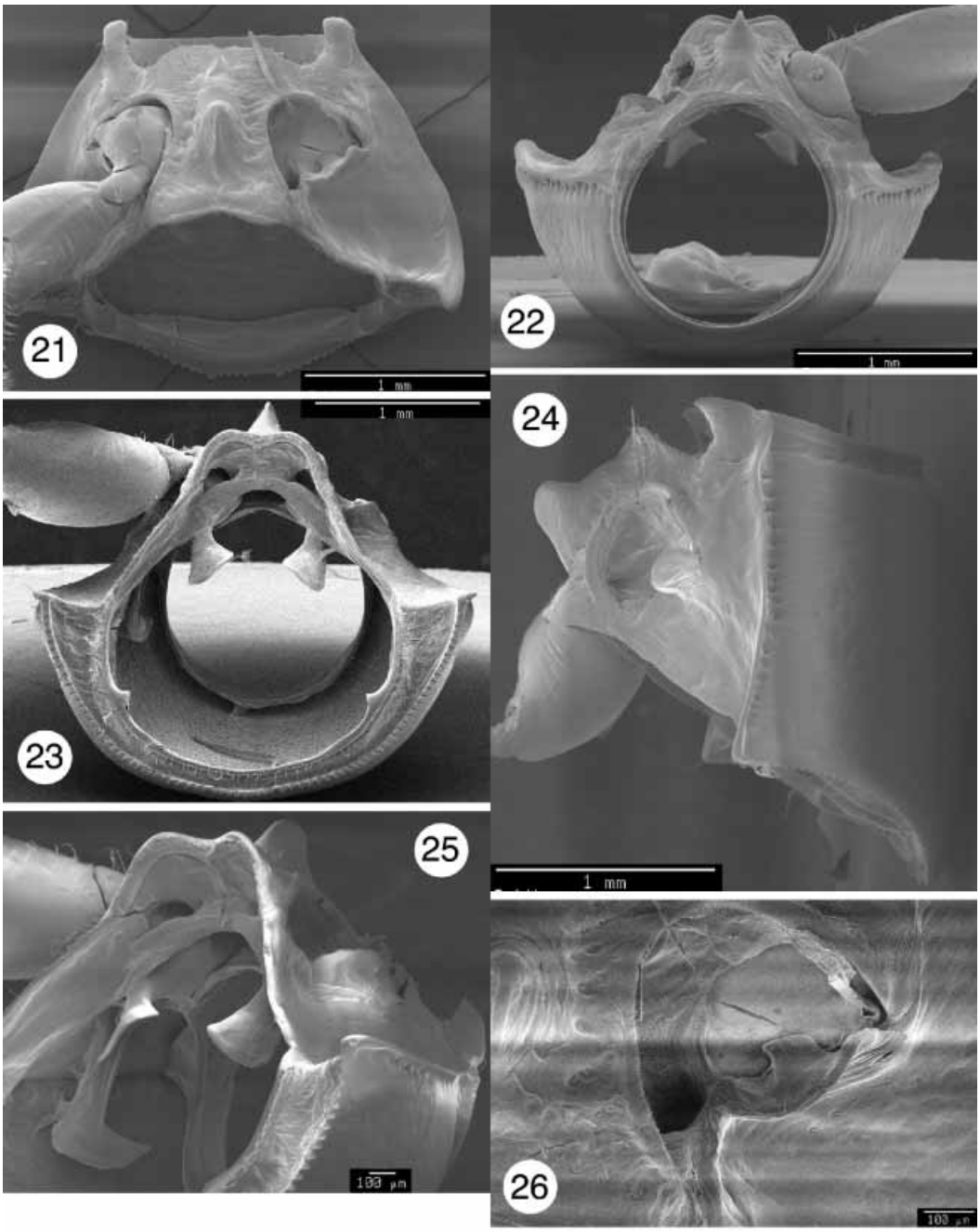

FIGURES 21–26. *Bassareus brunnipes*. 21, Ventral view of prothorax. 22, Anterior view. 23, Caudal view. 24, Lateral view. 25, Oblique caudal view and endopleuron. 26, Ventral view of coxal cavity.

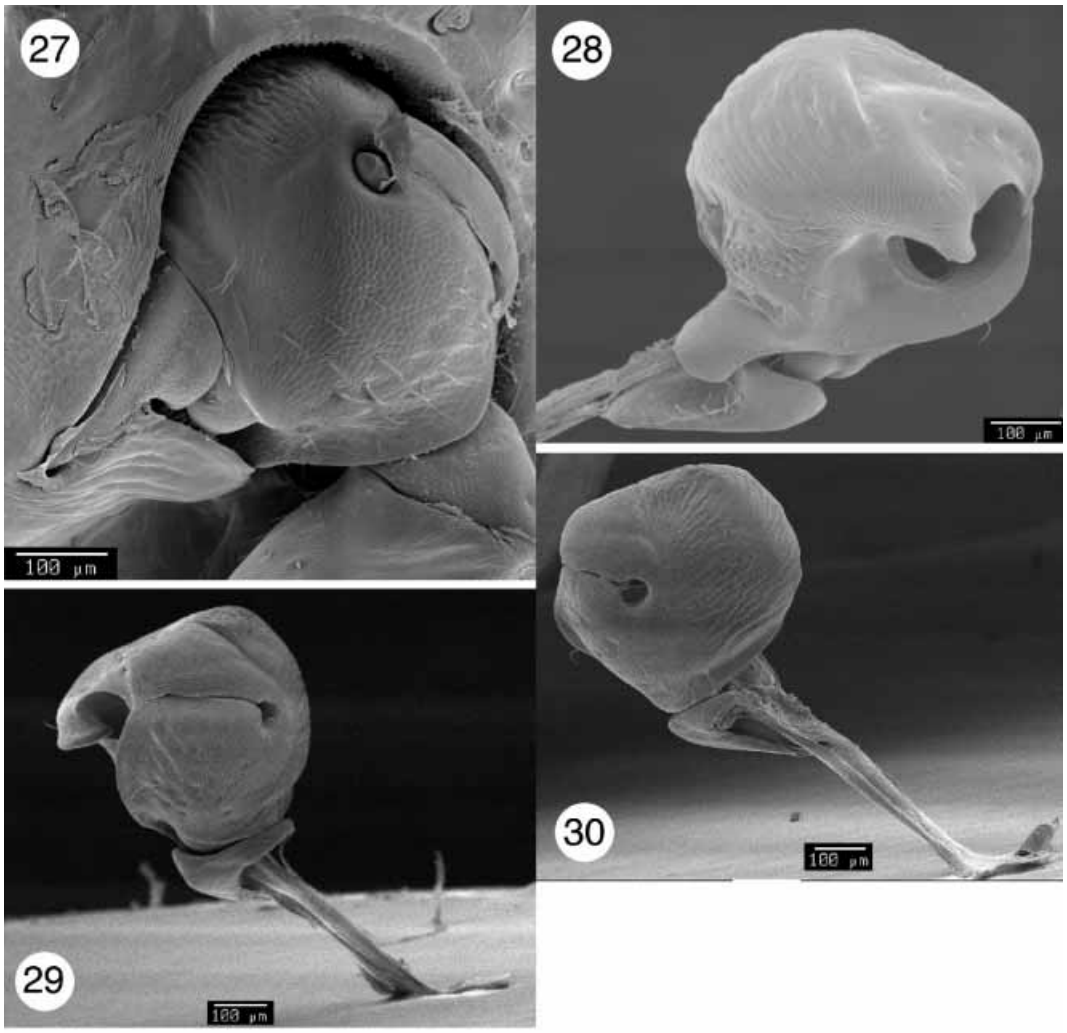

FIGURES 27–30. *Bassareus brunnipes*. 27, Ventral view of coxa inserted into cavity with attached trochantin and inserted trochanter. 28, Ventral aspect of coxa and trochantin. 29, Views of dorsal and ventral openings of coxa. 30, Dorsal aspect of coxa and trochantin.

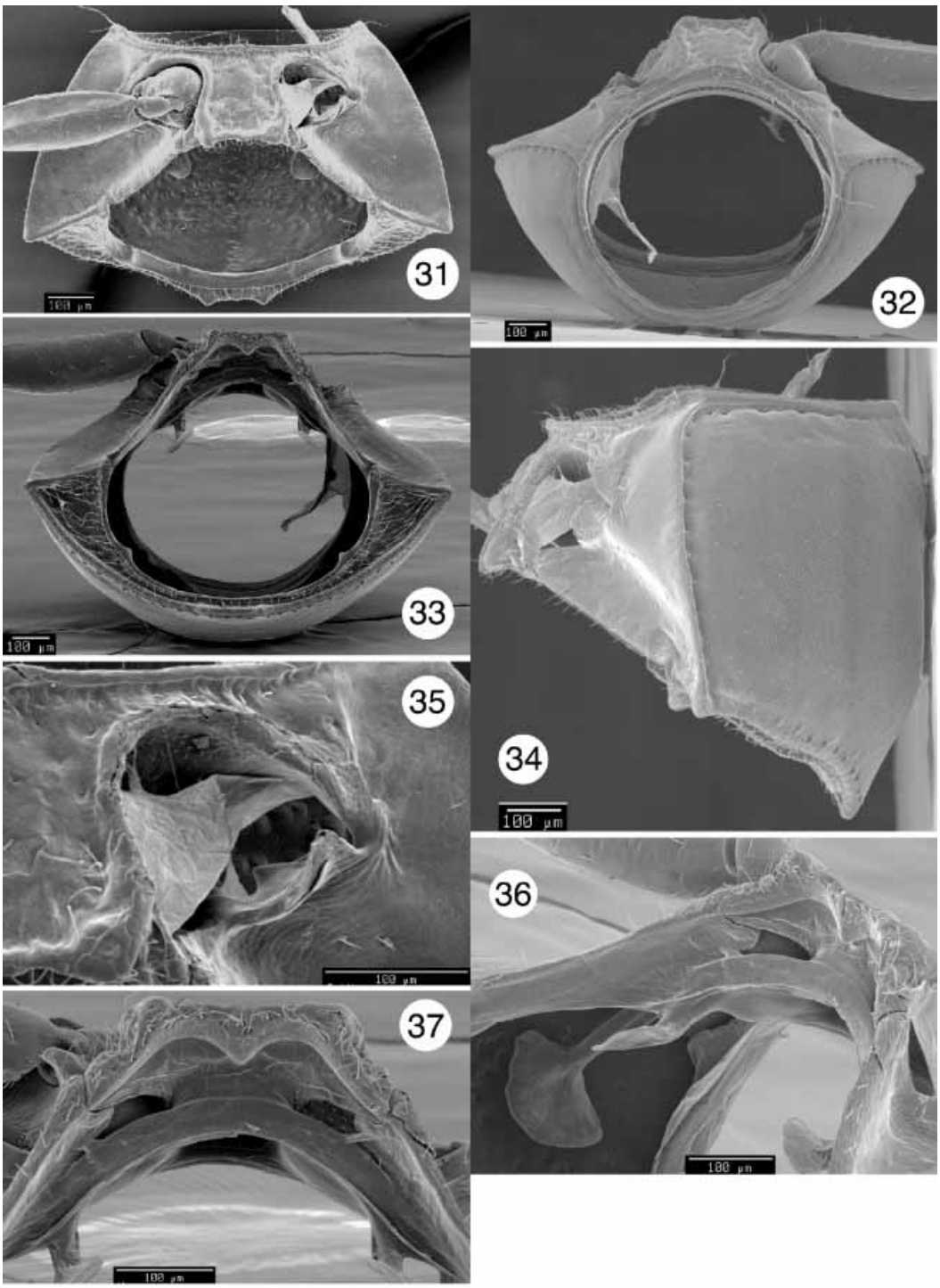

FIGURES 31–37. *Diachus auratus*. 31, Ventral view of prothorax. 32, Anterior view. 33, Caudal view. 34, Lateral view. 35, Ventral view of coxal cavity. 36, Oblique caudal view and endopleuron. 37, Caudal view of intercoxal prosternal process and sternacosta.

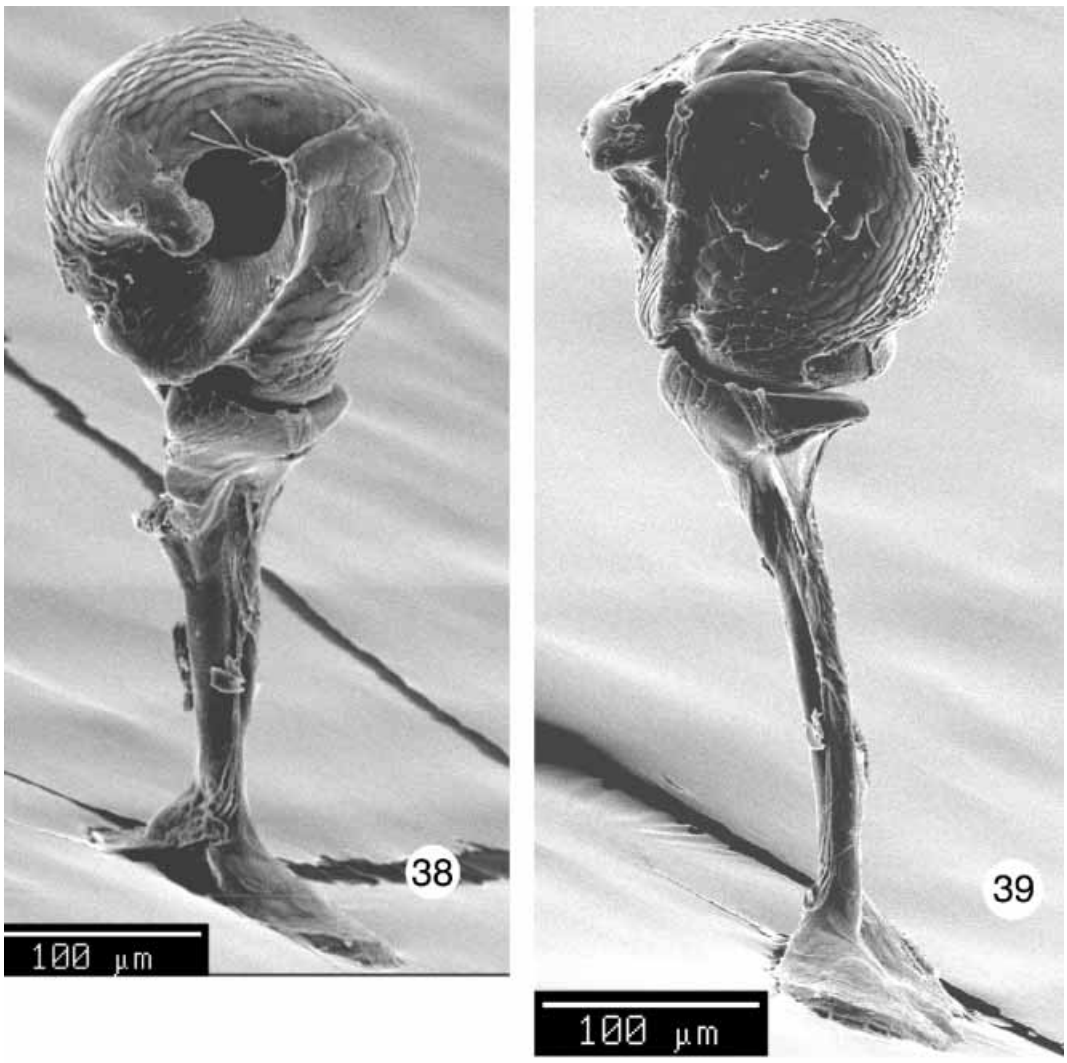

FIGURES 38–39. *Diachus auratus*. 38, View of ventral aspect of coxa, trochantin, and endopleuron. 39, View of coxal openings, trochantin, and endopleuron.

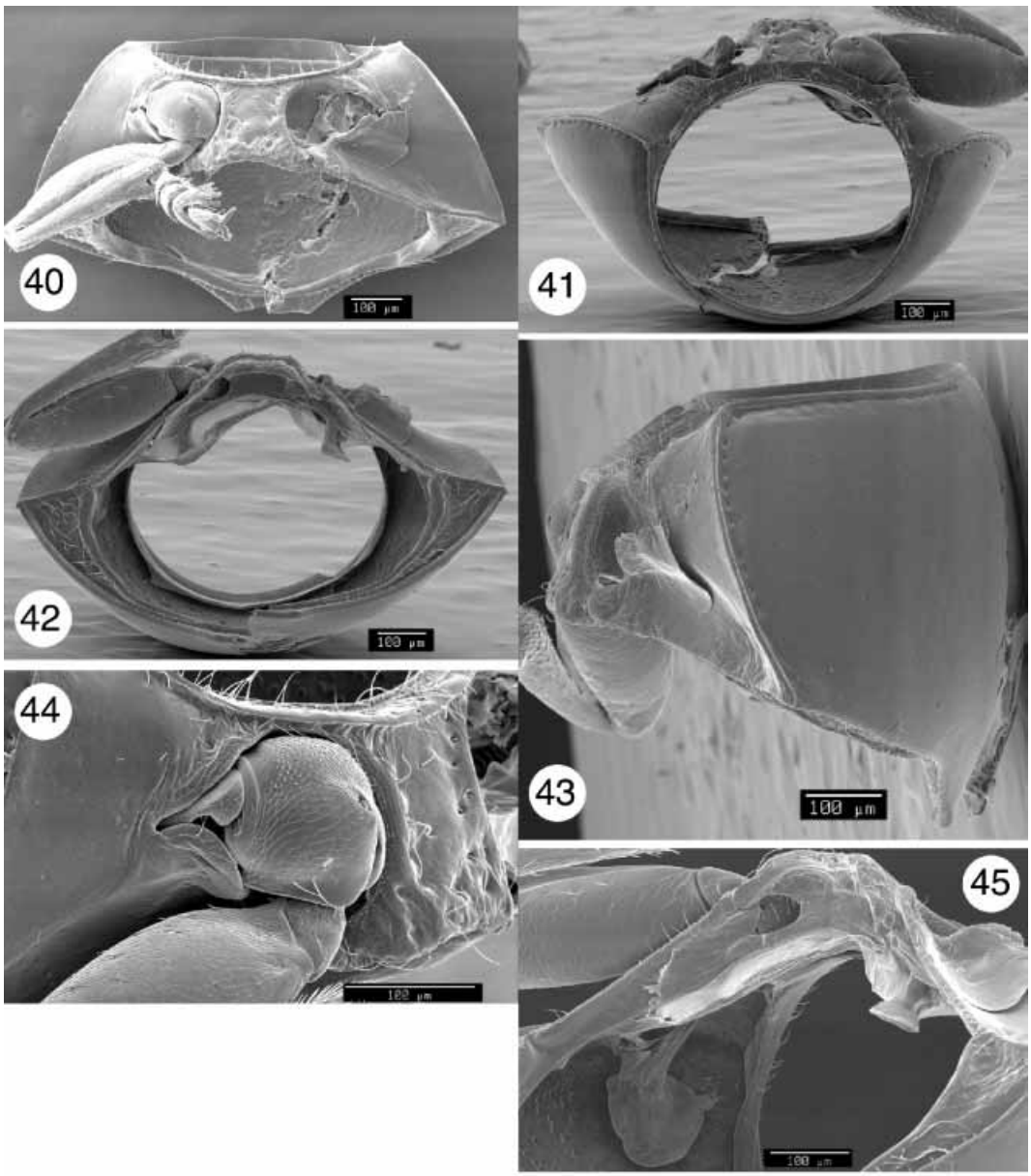

FIGURES 40–45. *Triachus vacuus*. 40, Ventral view of prothorax. 41, Anterior view. 42, Caudal view. 43, Lateral view. 44, Ventral view of coxa inserted into cavity with attached trochantin and inserted trochanter. 45, Oblique caudal view and endopleuron.

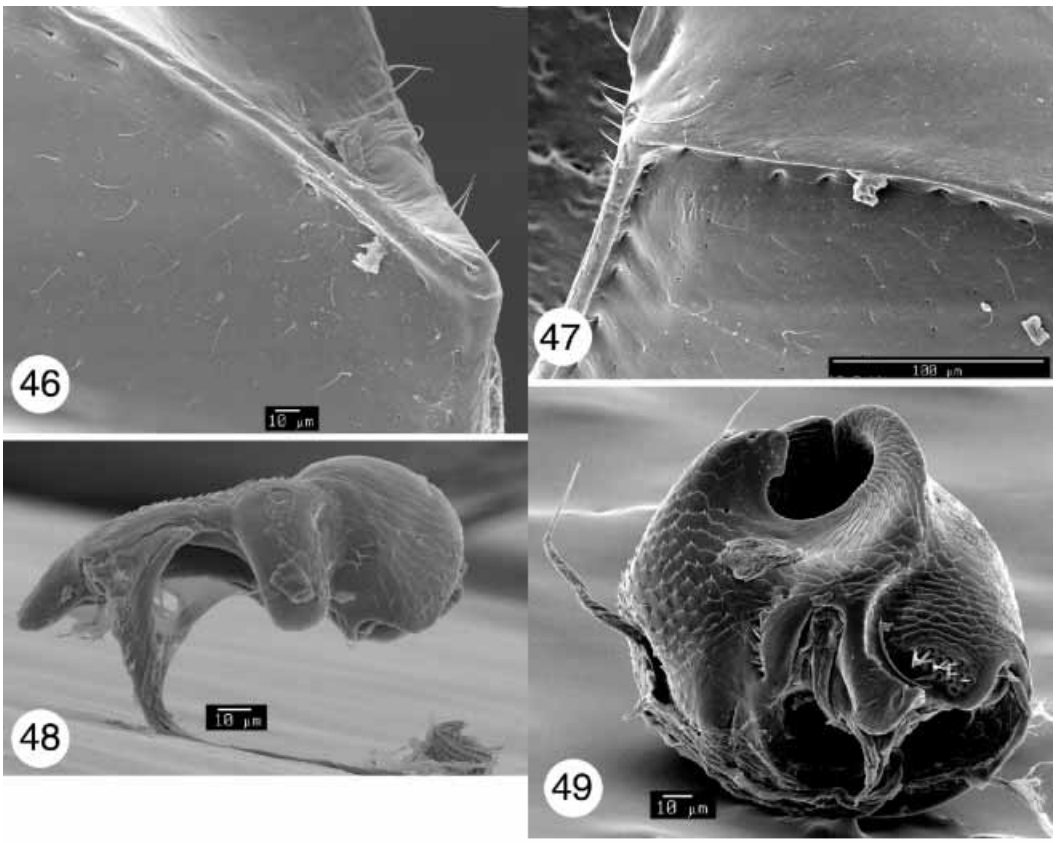

FIGURES 46–49. *Triachus vacuus*. 46, Detail of posterolateral prothoracic margin. 47, Detail of anterolateral margin and punctation. 48, Trochanter. 49, View of ventral coxal opening, lateral projection, proprioreceptive organ, in caudal view.

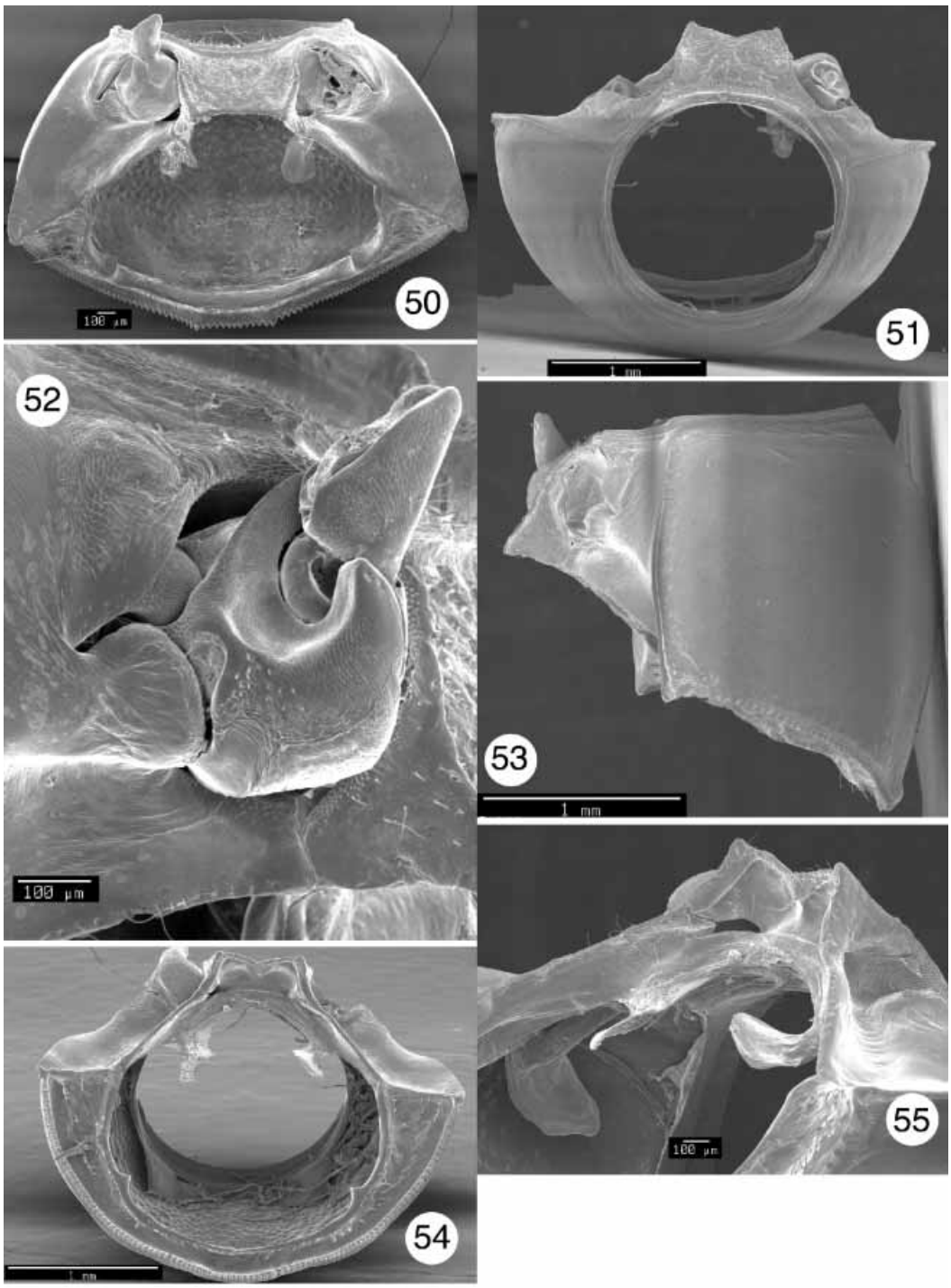

FIGURES 50–55. *Heptarthrius longimanus*. 50, Ventral view of prothorax. 51, Anterior view. 52, Inserted coxa. 53, Lateral view of prothorax 54, Caudal view. 55, Oblique caudal view and endopleuron.

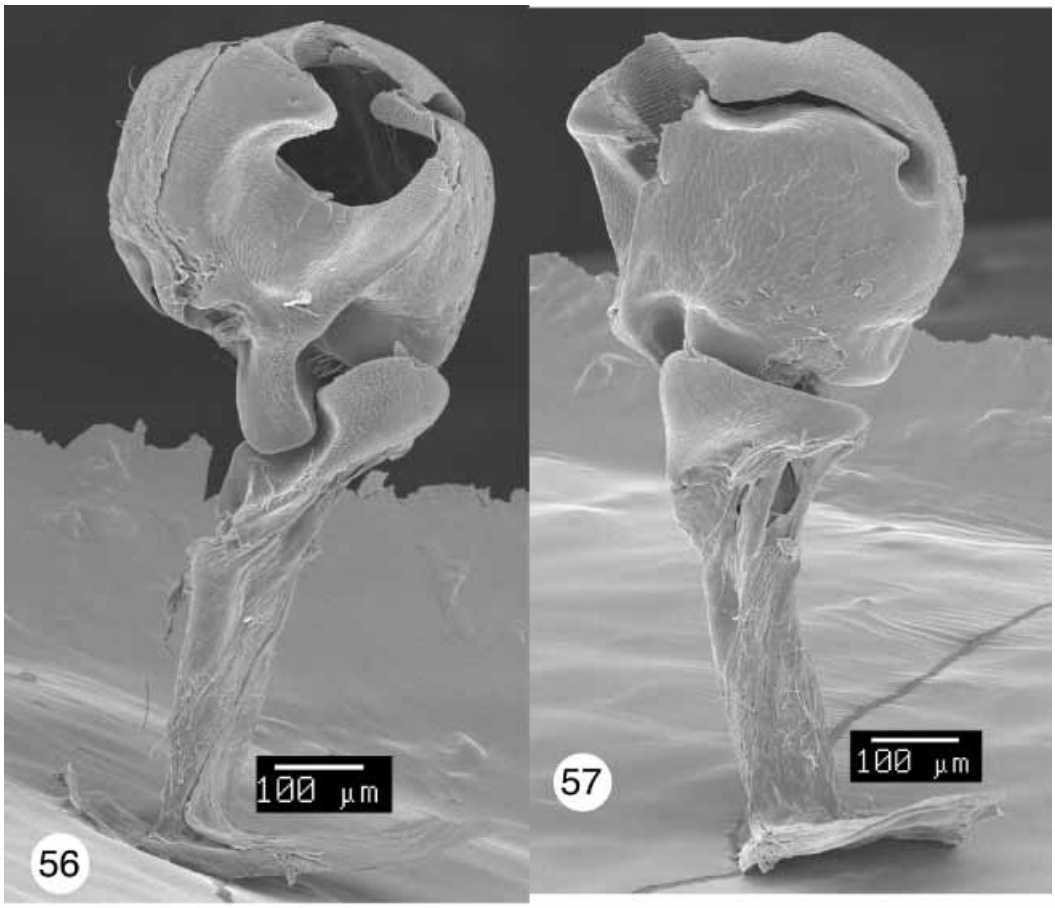

FIGURES 56–57. *Heptarthrius longimanus*. 56, View of ventral aspect of coxa, trochantin, endopleuron, and proprioreceptive organ. 57, View of coxal openings, trochantin, and endopleuron.

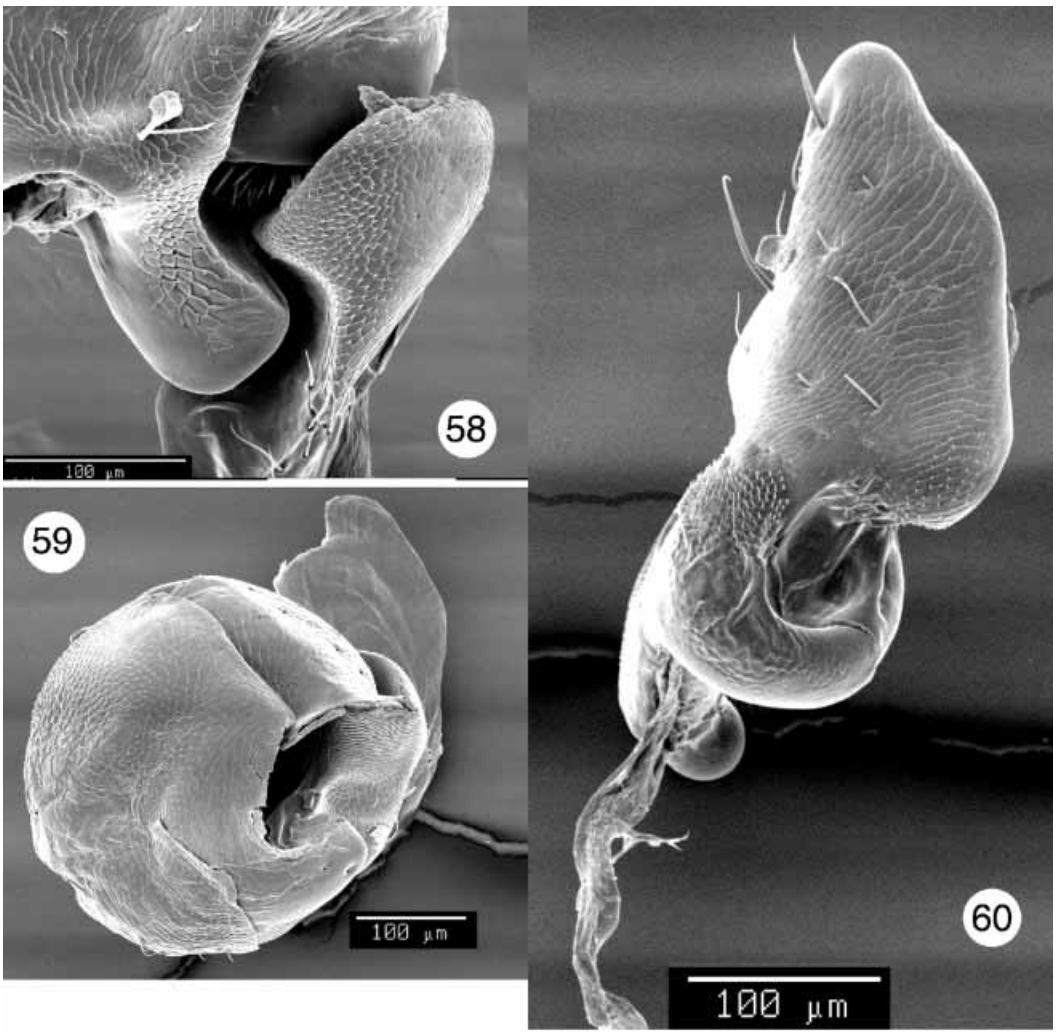

FIGURES 58–60. *Heptarthrius longimanus*. 58, View of posterior projection and proprioceptive organ. 59, Dorsal view of medial aspect of coxa. 60, Trochanter and tendon.

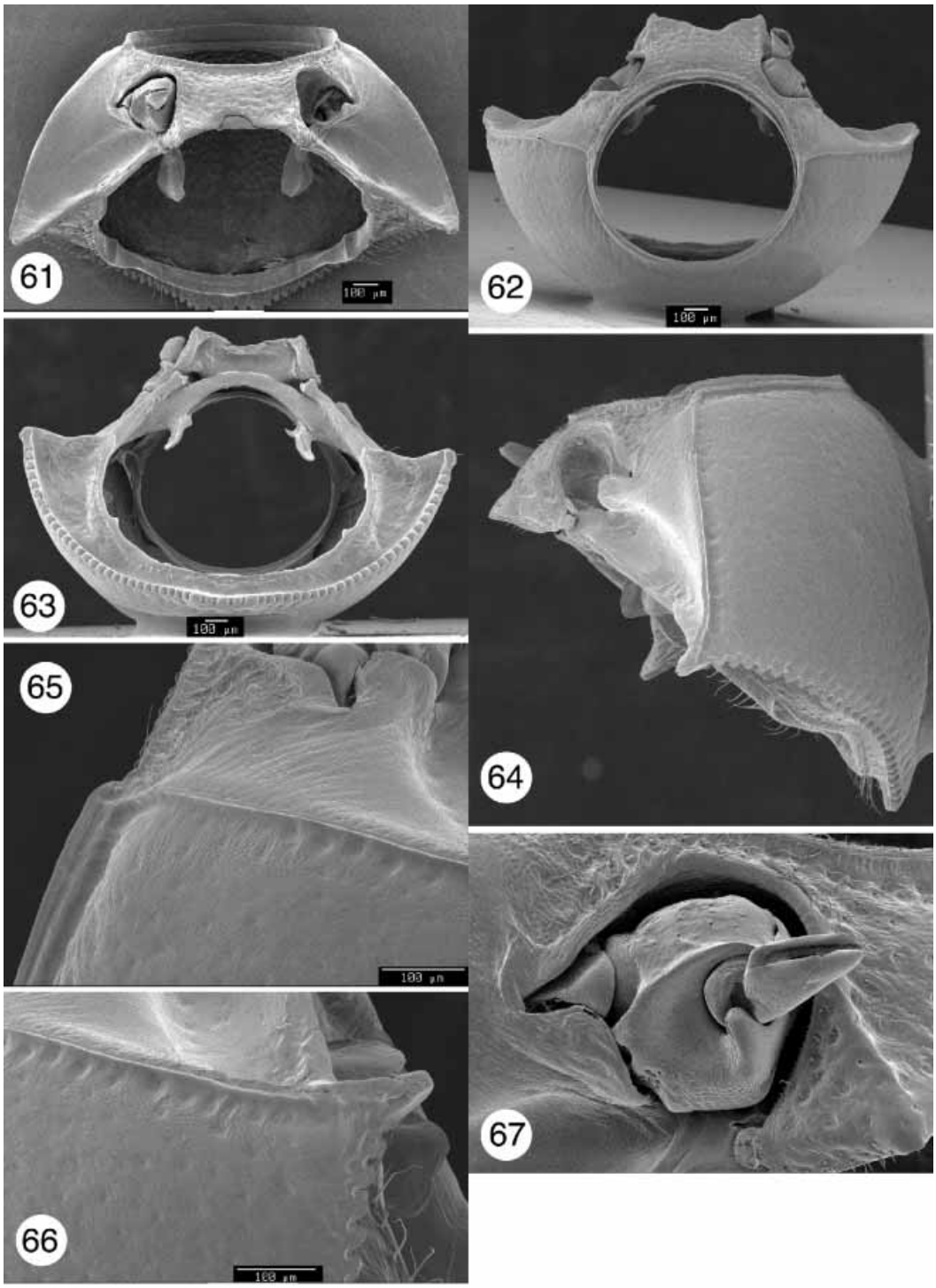

FIGURES 61–67. *Lexiphanes coenobita*. 61, Ventral view of prothorax. 62, Anterior view. 63, Caudal view. 64, Lateral view. 65, Detail of anterolateral prothoracic margin. 66, Detail of posterolateral margin. 67, Inserted coxa with trochantin and trochanter.

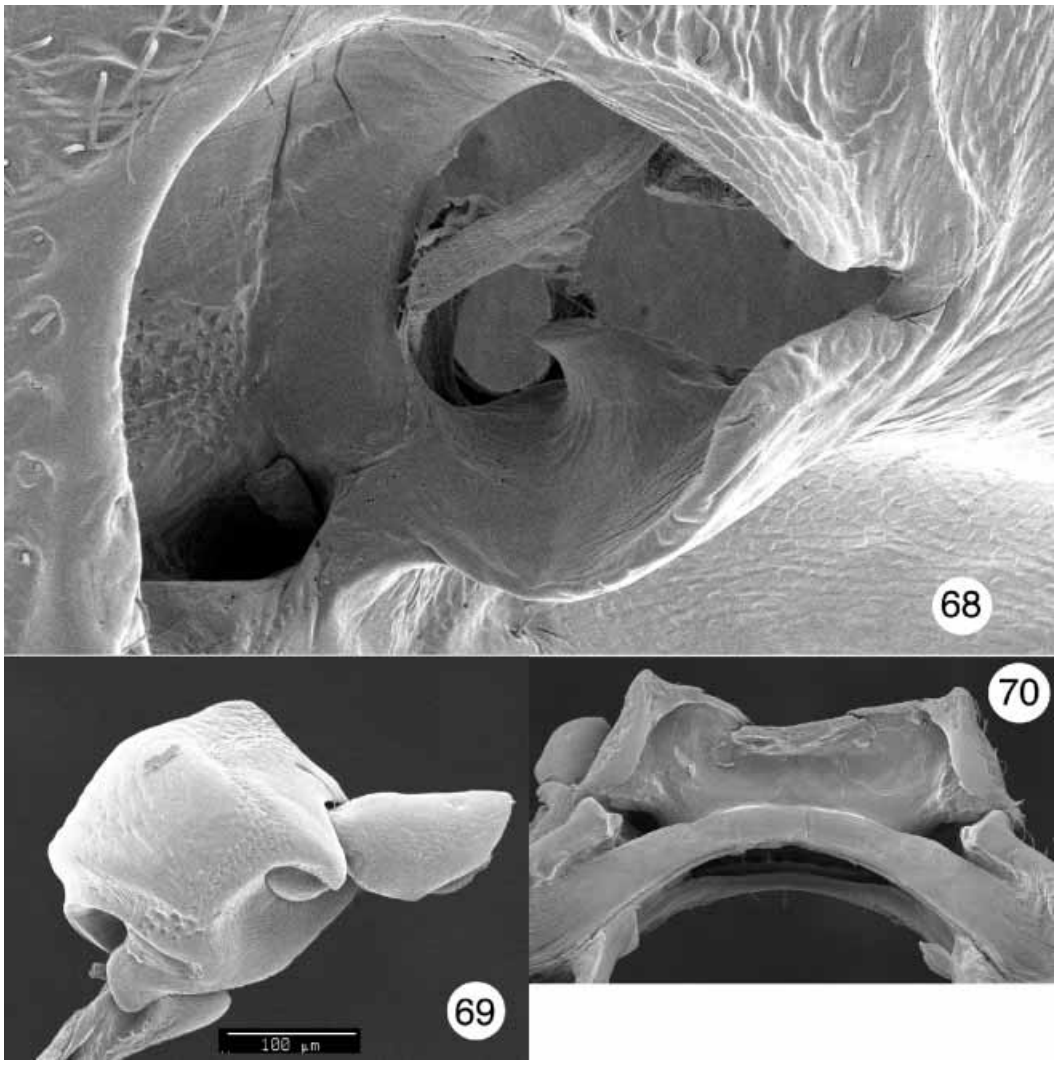

FIGURES 68–70. *Lexiphanes coenobita*. 68, Ventral view of coxal cavity. 69, Coxa with inserted trochanter and attached trochantin. 70, Intercoxal prosternal process and sternacosta.

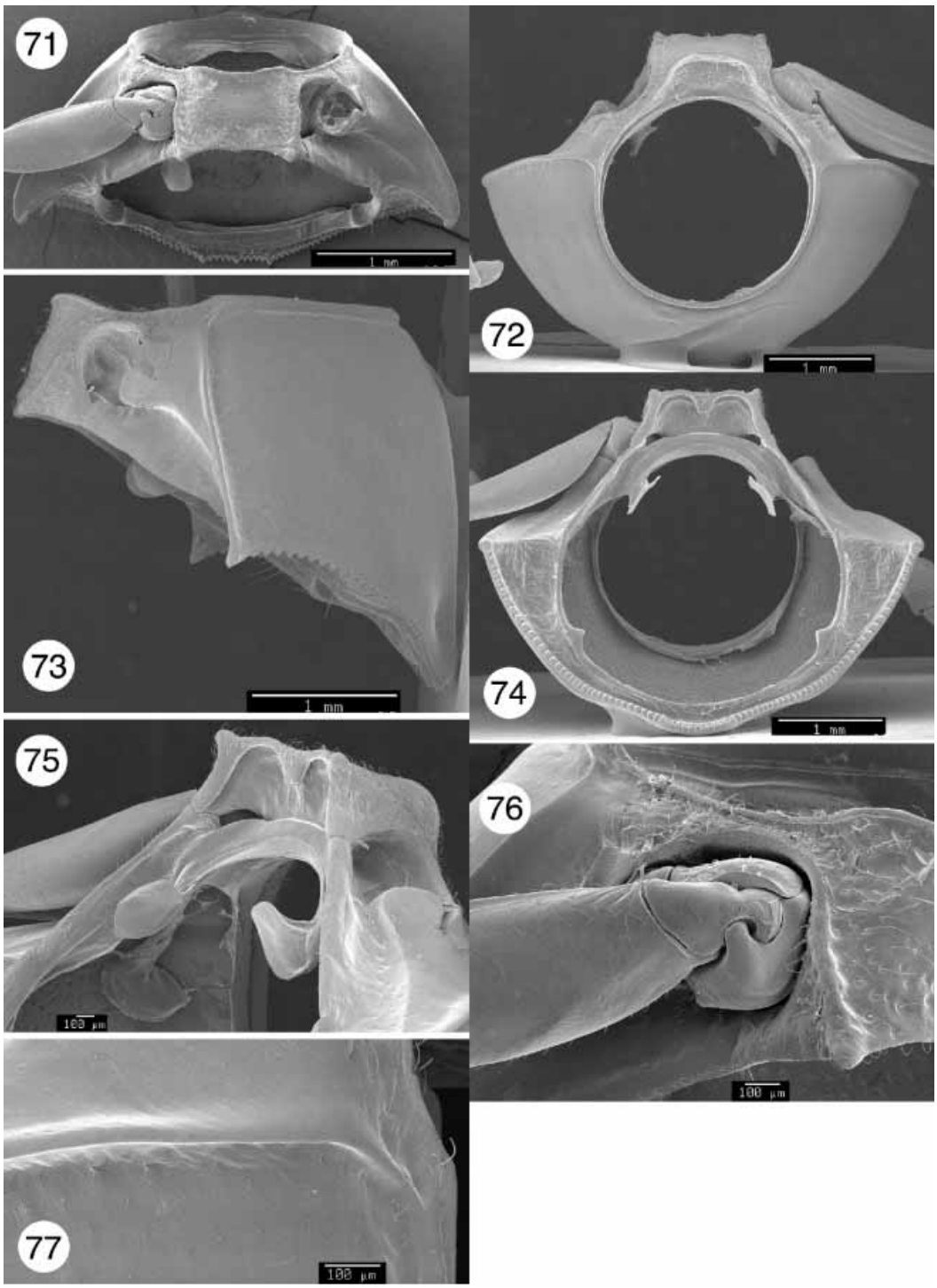

FIGURES 71–77. *Stegnocephala costulata*. 71, Ventral view of prothorax. 72, Anterior view. 73, Lateral view. 74, Caudal view. 75, Oblique caudal view and endopleuron. 76, Inserted coxa with attached trochanter. 77, Detail of lateral prothoracic margin.

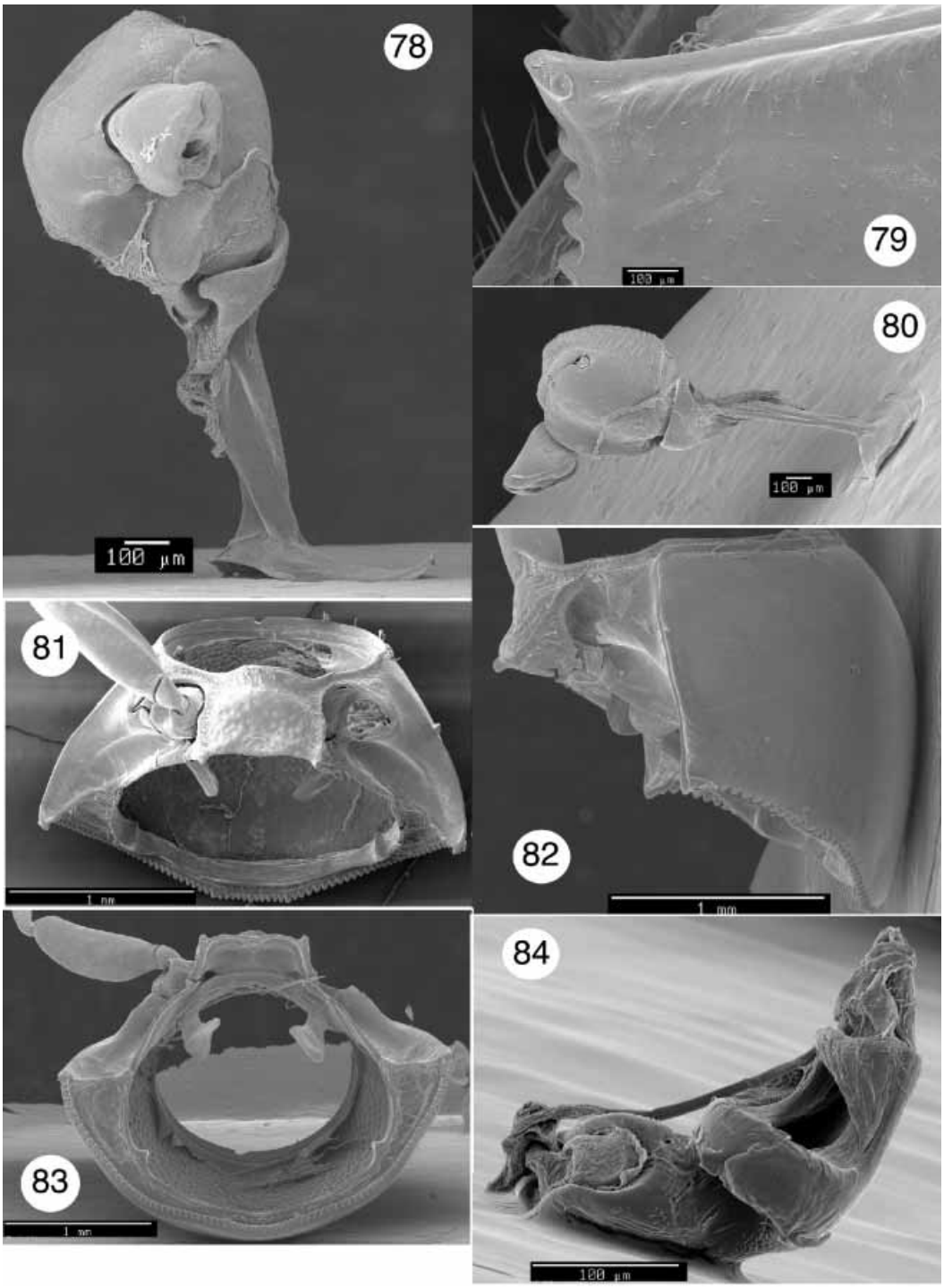

FIGURES 78–80. *Stegnocephala costulata*. 78, View of ventral aspect of coxa with inserted trochanter, attached trochantin and endopleuron. 79, Detail of lateral prothoracic margin. 80, View of dorsal aspect of coxa with inserted trochanter, attached trochantin and endopleuron. **FIGURES 81–84.** *Stegnocephala discoidalis*. 81, Ventral view of prothorax. 82, Lateral view. 83, Caudal view. 84, Trochanter.

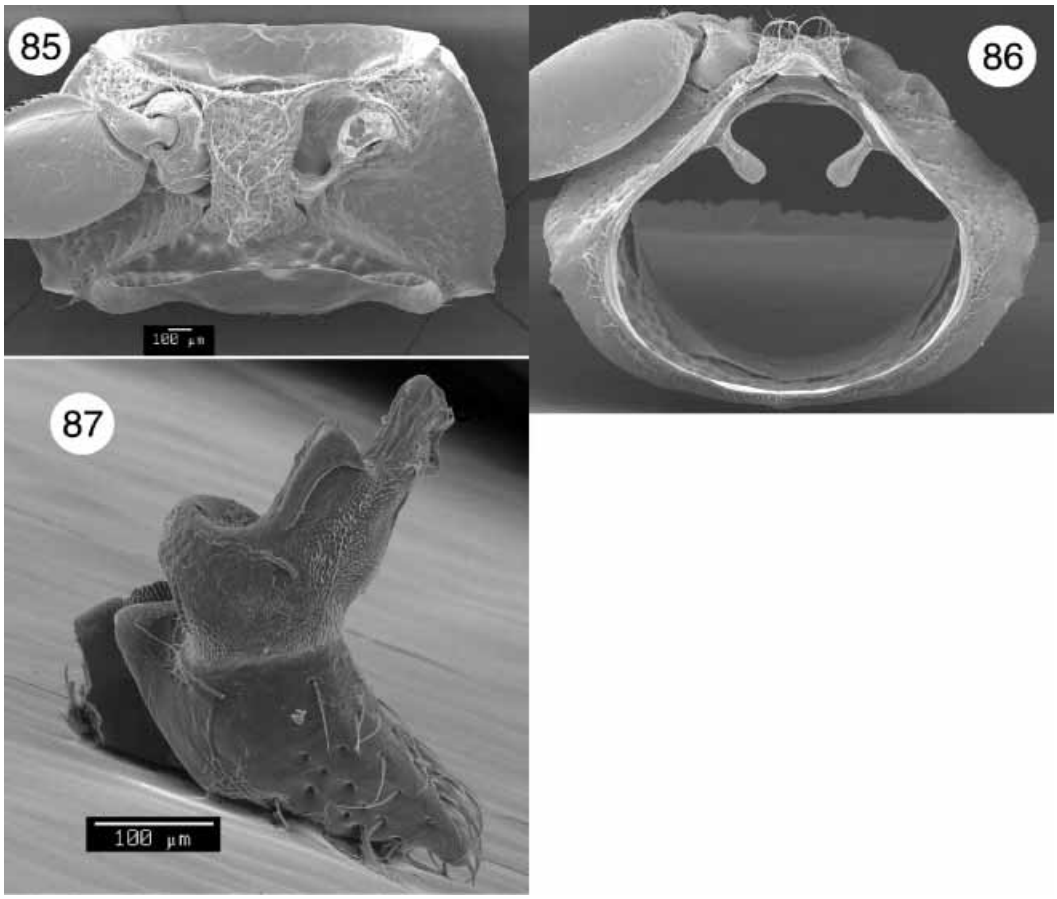

FIGURES 85–87. *Pachybrachis gayi*. 85, Ventral view of prothorax. 86, Caudal view. 87, Trochanter.

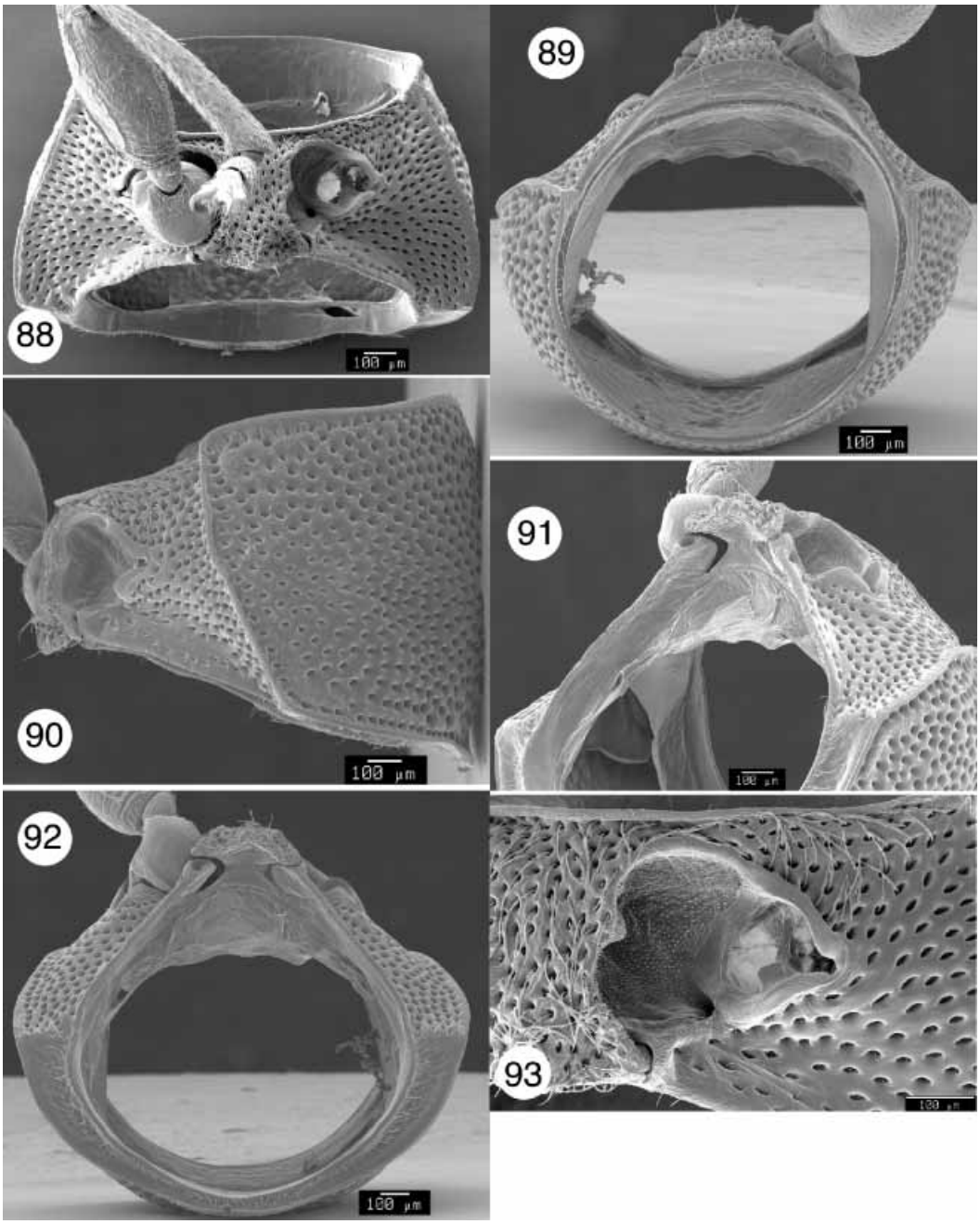

FIGURES 88–93. *Pachybrachis hepaticus*. 88, Ventral view of prothorax. 89, Anterior view. 90, Lateral view. 91, Oblique caudal view and endopleuron. 92, Caudal view of prothorax, proendosternites lost during dissection process. 93, Ventral view of coxal cavity.

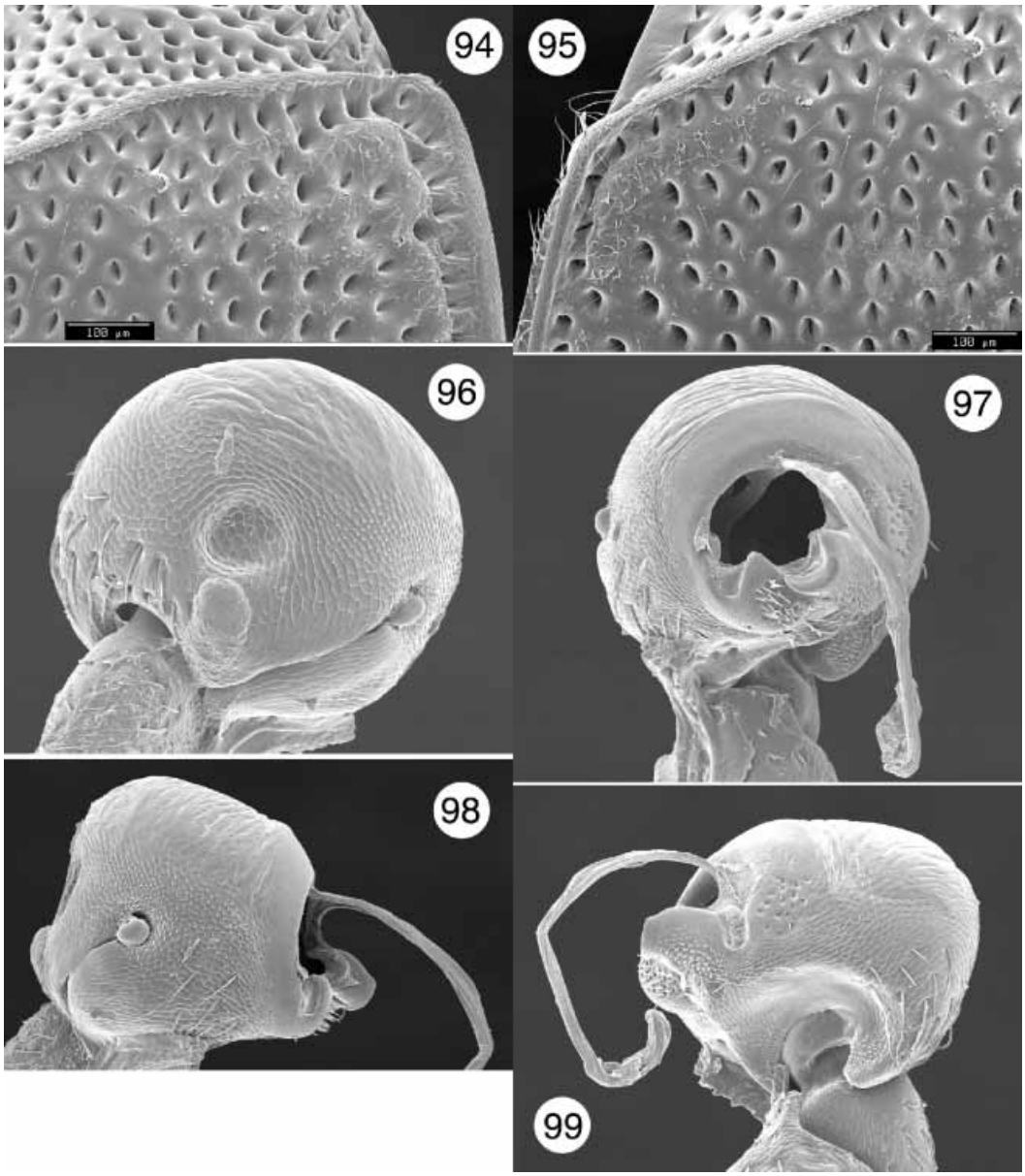

FIGURES 94–99. *Pachybrachis hepaticus*. 94, Detail of anterolateral prothoracic margin. 95, Detail of posterolateral margin and punctation. 96, Coxal suture with inserted trochanter, anterior aspect. 97, Caudal view of coxa and lateral projection, opening for trochantin-endopleuron insertion. 98, View of dorsal opening with trochanter inserted and view of tendon. 99, View of ventral aspect and lateral projection.

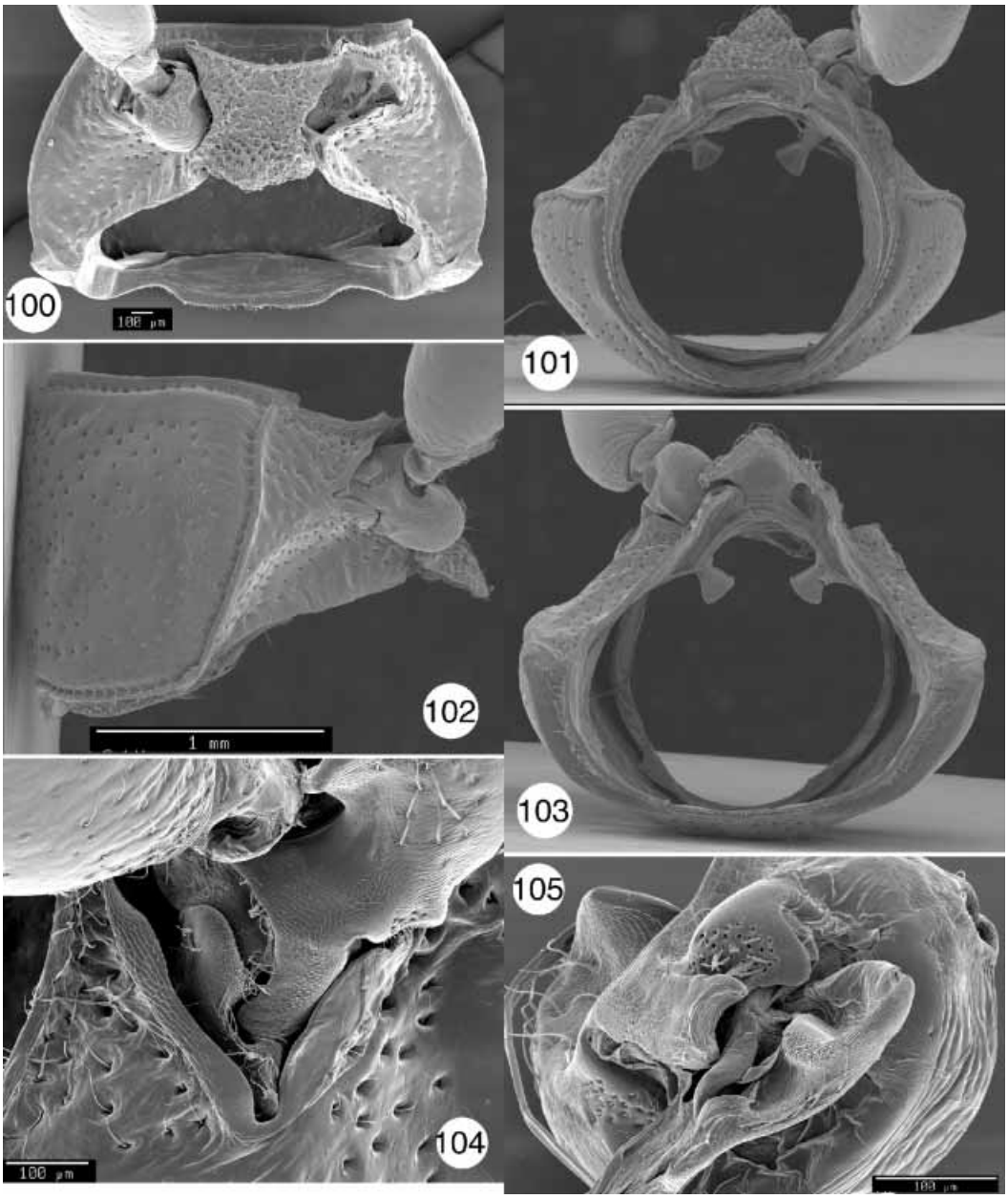

FIGURES 100–105. *Metallactus decumanus*. 100, Ventral view of prothorax. 101, Anterior view. 102, Lateral view. 103, Caudal view (dissection poor). 104, Coxa inserted into coxal cavity, view of lateral projection of coxa and attached trochantin 105, Caudal view of coxa with partially detached trochantin, view of proprioreceptive organ.

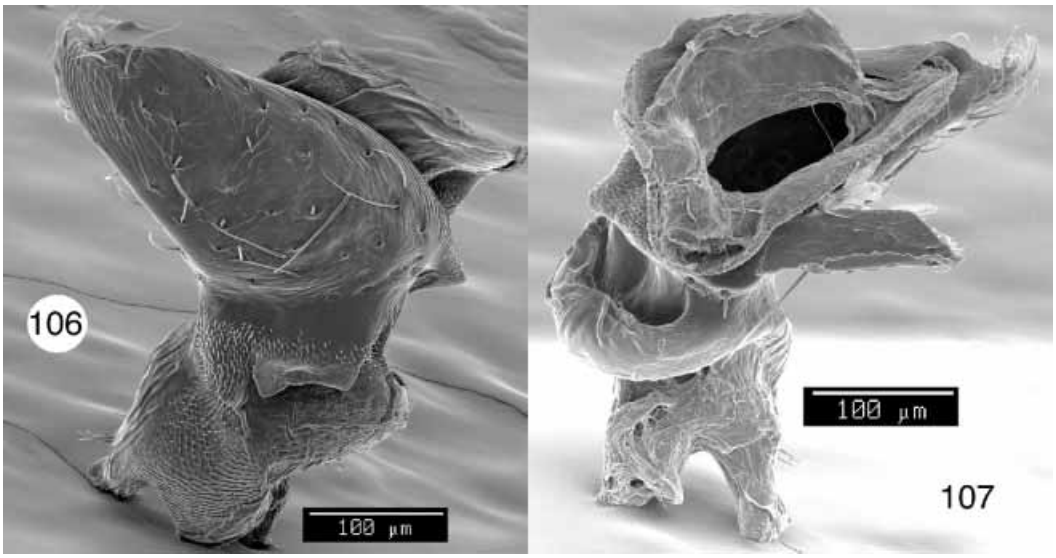

FIGURES 106–107. *Metallactus decumanus*. 106, Trochanter. 107, View of spiral ridge of trochanter.

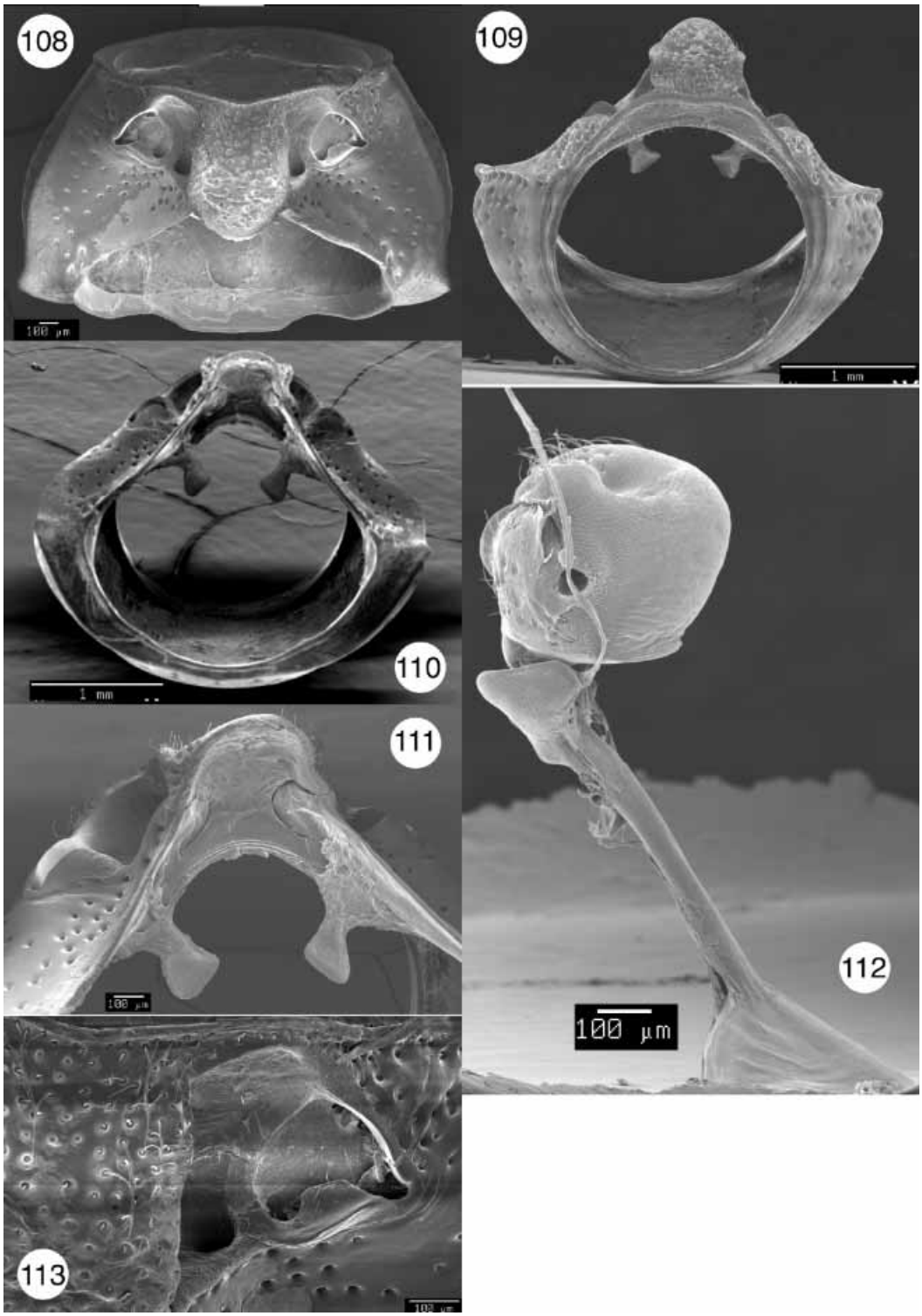

FIGURES 108–113. *Griburius sp*. 108, Ventral view of prothorax. 109, Anterior view. 110, Caudal view. 111, Slightly oblique caudal view. 112, Dorsal aspect of coxa, with attached trochanter, trochantin and endopleuron. 113, Ventral view of coxal cavity.

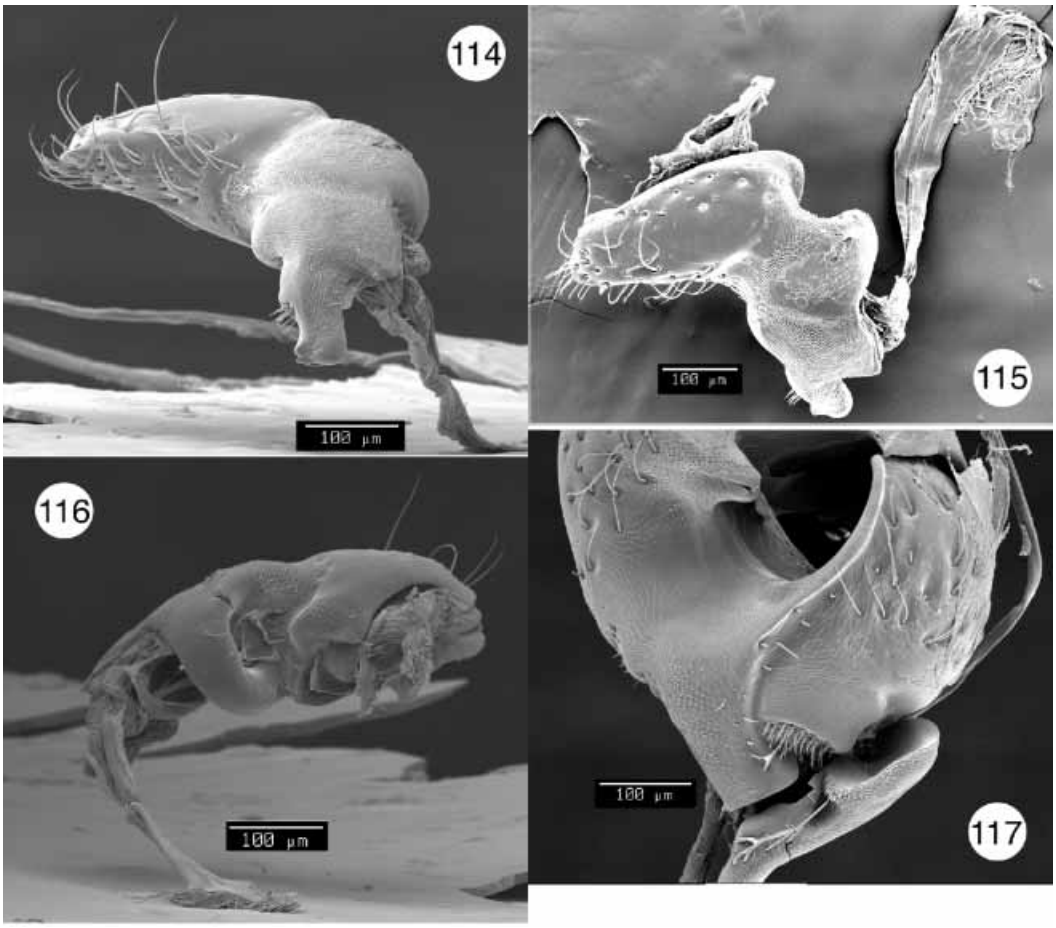

FIGURES 114–117. *Griburius sp.* 114, 115, Trochanter. 116, Spiral ridge of trochanter and tendon. 117, View of ventral opening of coxa, lateral projection, trochantin, and proprioceptive organ.

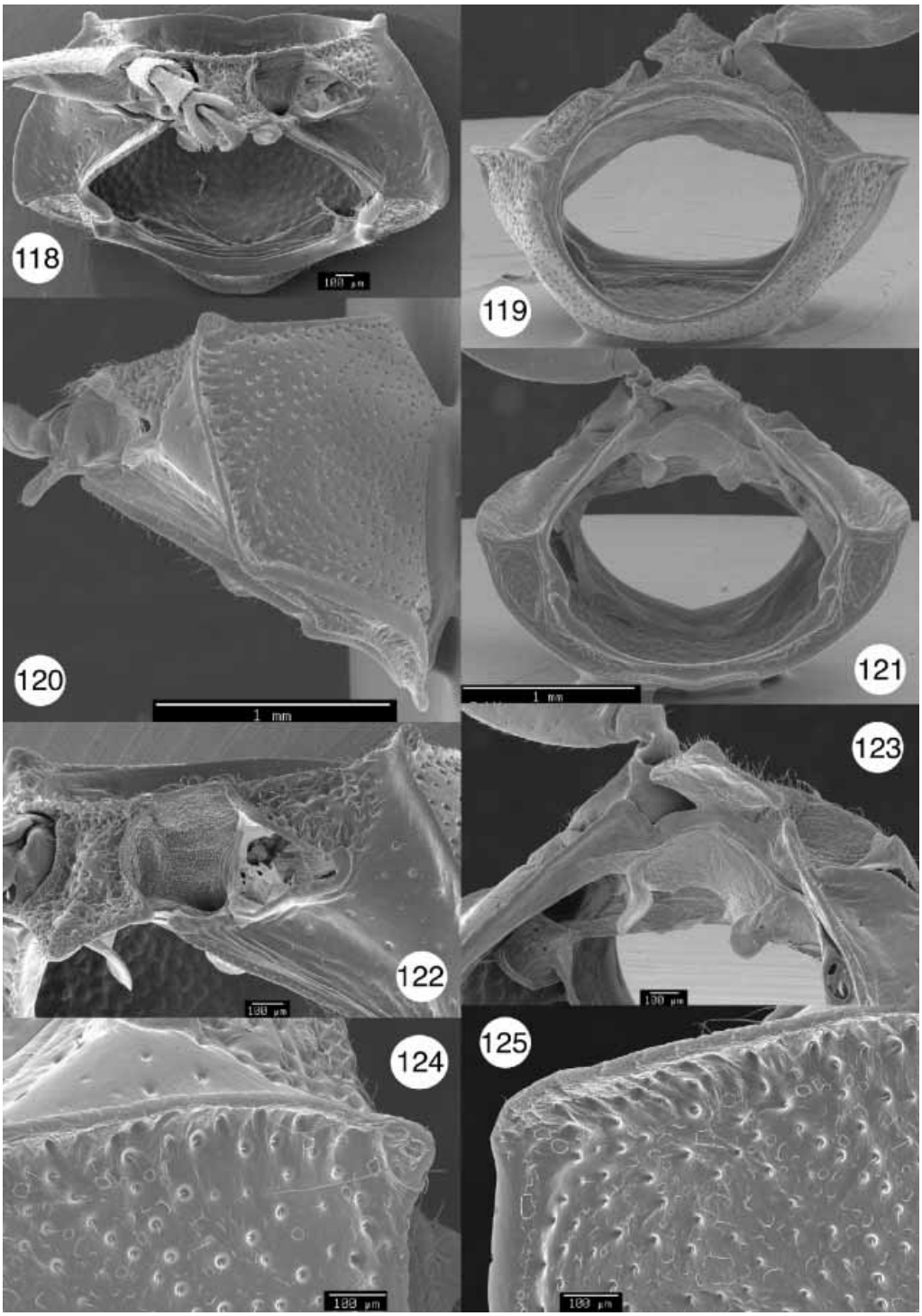

FIGURES 118–125. *Ambrotodes chilensis*. 118, Ventral view of prothorax. 119, Anterior view. 120, Lateral view. 121, Caudal view. 122, Ventral view of coxal cavity. 123, Oblique caudal view and endopleuron. 124, Detail of anterolateral prothoracic margin. 125, Detail of posterolateral margin and punctations.

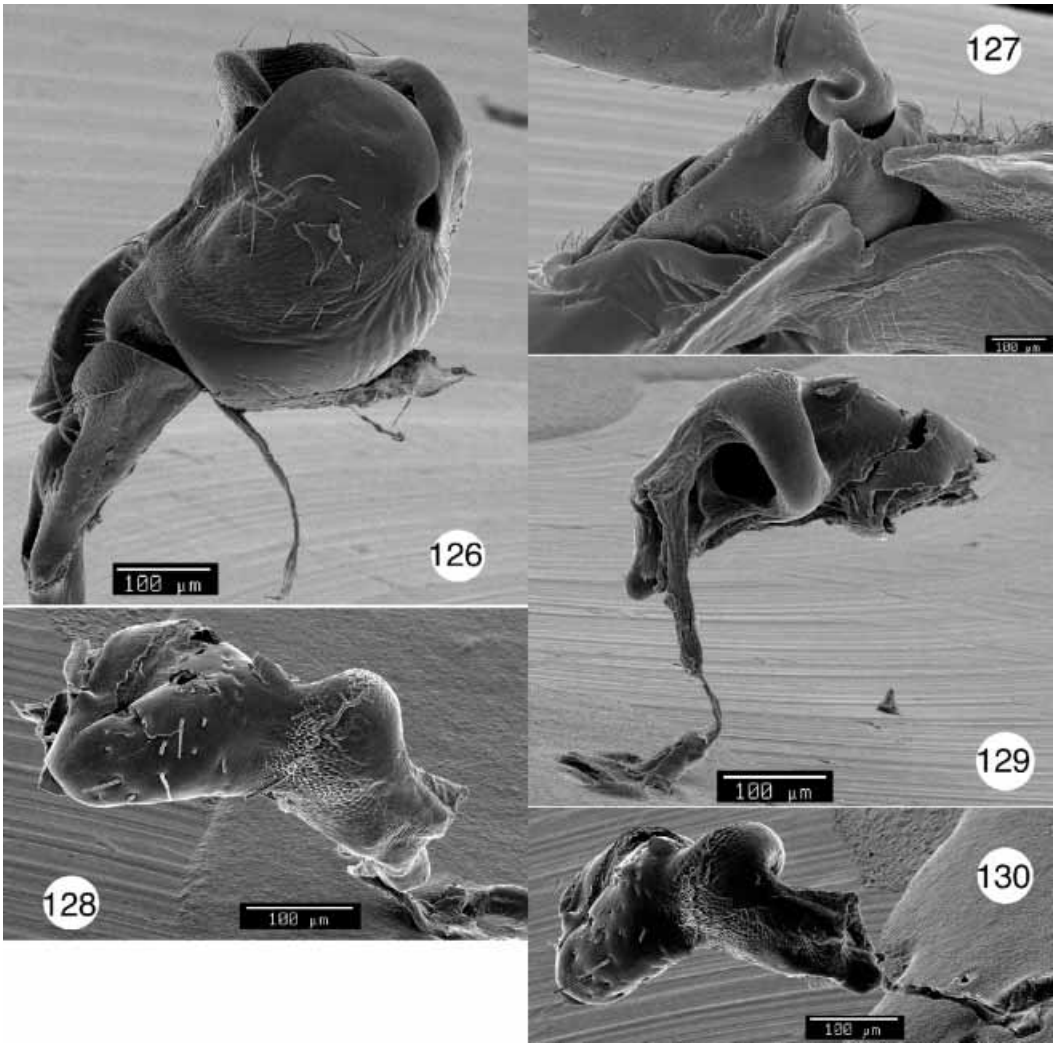

FIGURES 126–130. *Ambrotodes chilensis*. 126, View of dorsal opening and dorsal aspect of coxa. 127, Inserted coxa and trochanter showing spiral ridge. 128, Trochanter. 129, Spiral ridge of trochanter and tendon. 130, Trochanter.

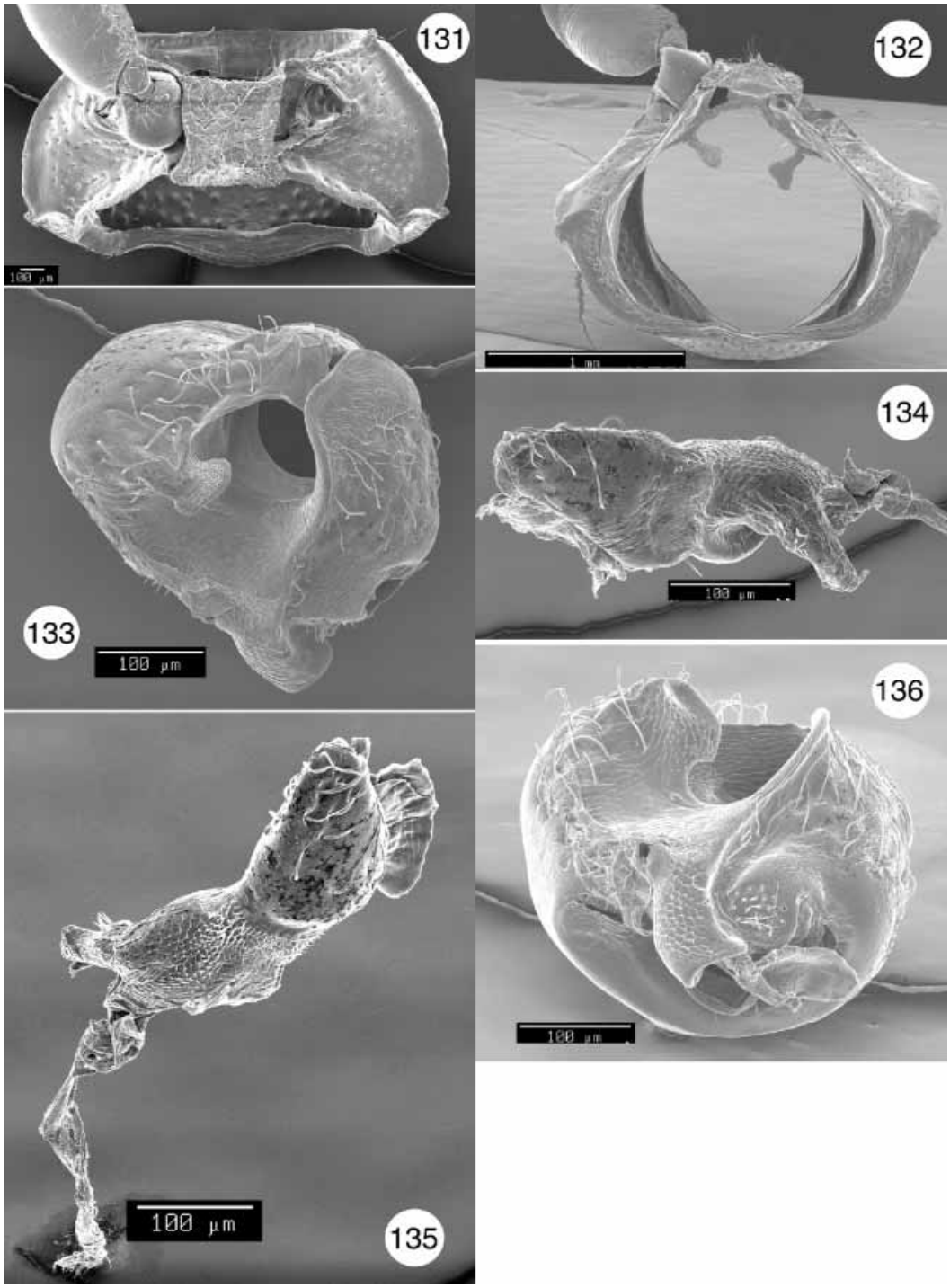

FIGURES 131–136. *Ambrotodes signatipennis*. 131, Ventral view of prothorax. 132, Caudal view. 133, View of posterior projection and ventral opening of coxa. 134, 135, Trochanter.136, View of lateral aspect and lateral projection of coxa.

